Impact of Physics Representations in the HWRFX on Simulated Hurricane Structure and Pressure–Wind Relationships

J.-W. Bao

NOAA/ESRL, Boulder, Colorado

S. G. Gopalakrishnan

NOAA/AOML, Miami, Florida

S. A. Michelson

NOAA/ESRL, and CIRES Climate Diagnostics Center, University of Colorado, Boulder, Colorado

F. D. Marks

NOAA/AOML, Miami, Florida

M. T. Montgomery

NOAA/AOML, Miami, Florida, and Naval Postgraduate School, Monterey, California

ABSTRACT

A series of idealized experiments with the NOAA Experimental Hurricane Weather Research and Forecasting Model (HWRFX) are performed to examine the sensitivity of idealized tropical cyclone (TC) intensification to various parameterization schemes of the boundary layer (BL), subgrid convection, cloud microphysics, and radiation. Results from all the experiments are compared in terms of the maximum surface 10-m wind (VMAX) and minimum sea level pressure (PMIN)—operational metrics of TC intensity—as well as the azimuthally averaged temporal and spatial structure of the tangential wind and its material acceleration.

The conventional metrics of TC intensity (VMAX and PMIN) are found to be insufficient to reveal the sensitivity of the simulated TC to variations in model physics. Comparisons of the sensitivity runs indicate that (i) different boundary layer physics parameterization schemes for vertical subgrid turbulence mixing lead to differences not only in the intensity evolution in terms of VMAX and PMIN, but also in the structural characteristics of the simulated tropical cyclone; (ii) the surface drag coefficient is a key parameter that controls the VMAX–PMIN relationship near the surface; and (iii) different microphysics and subgrid convection parameterization schemes, because of their different realizations of diabatic heating distribution, lead to significant variations in the vortex structure.

The quantitative aspects of these results indicate that the current uncertainties in the BL mixing, surface drag, and microphysics parameterization schemes have comparable impacts on the intensity and structure of simulated TCs. The results also indicate that there is a need to include structural parameters in the HWRFX evaluation.

1. Introduction

The structure and intensification of tropical cyclones (TCs) as simulated by numerical models are found to be quite sensitive to the details in the physics parameterizations (e.g., Hausman 2001). A recent study conducted by Smith and Thomsen (2010) showed that the prediction of tropical cyclone intensification is sensitive to the variations in the boundary layer (BL) physics schemes. Specifically, the onset time of rapid intensification, the low-level wind structure in the eyewall region, and the overall intensity after a few days of

numerical integration are sensitive to the differences in the determination of the vertical eddy diffusivity in the model. In addition to the sensitivity to the vertical eddy diffusivity, Smith et al. (2011, manuscript submitted to *Quart. J. Roy. Meteor. Soc.*) found that the change in the model-simulated tropical cyclone intensification is sensitive to the surface drag coefficient, but this sensitivity depends also on the BL scheme used. The prediction of tropical cyclone intensification has also been shown to be sensitive to the treatment of the physics in resolved and unresolved convective clouds (Zhu and Smith 2002).

Observations and modeling studies are beginning to provide a consistent picture of the tropical cyclone intensification process in which deep convective features growing in the rotation-rich environment of the incipient vortex core amplify the local vertical rotation. These deep convective features have been suggested to be the basic coherent structures of the intensification process, which itself is intrinsically asymmetric and possesses a stochastic component. Nguyen et al. (2008) found that the progressive segregation, merger, and axisymmetrization of these features and the low-level convergence they generate are fundamental to the intensification process. If this picture is correct, then a logical outcome is that the model-simulated tropical cyclone intensification and structure should be sensitive to small perturbations in the BL mixing of enthalpy and variations in the treatment of cloud physics (e.g., Wang 2002; Bryan and Rotunno 2009). However, it is still unclear which of these effects (BL mixing, surface drag, microphysics) has the most significant impact. The intrinsic sensitivity of numerically simulated intensification and structure of tropical cyclones to variations in model physics needs to be physically understood to meaningfully evaluate the quality of a numerical model's prediction using observations.

Historically, the maximum surface (10 m) wind (VMAX) and minimum sea level pressure (PMIN) of tropical cyclones are used as key parameters, along with the location of storm center, in the verification of operational tropical cyclone forecasts. They are also commonly used to evaluate numerical model performance. Observations from reconnaissance flights have produced statistically independent estimates of PMIN and VMAX. Such measurements are widely used to provide information on the pressure–wind relationship (PWR) for documenting tropical cyclones and evaluating operational prediction models (e.g., Koba et al. 1990; Harper 2002; Kossin and Velden 2004; Knaff and Zehr 2007; Holland 2008; Brown et al. 2010). It is widely accepted in the operational community that, despite large uncertainty in the datasets used in its derivation, the

PWR of tropical cyclones provides a statistically meaningful relationship between the surface pressure deficit between the environment and the center of the cyclone and the increase in the maximum surface wind around the cyclone.

The gradient-wind balance of an inviscid circular vortex is a three-way force balance in the radial direction between the pressure gradient, Coriolis, and centrifugal forces. This force balance is fundamental to intense geophysical vortices such as hurricanes. The gradient balance involves implicitly an important structural parameter, the radius of maximum wind (RMW), which is unfortunately less reliably observed than either VMAX or PMIN. The lack of reliable observations of the RMW in real hurricanes makes it difficult to relate the observed PWRs directly to the individual components composing the gradient-wind balance equation. Although the gradient-wind balance embedded in the observed PWRs appears to contain much of the essential dynamics of the vortex tangential wind above the BL, such a zero order balance relationship is not valid in the BL where the radial inflow is no longer negligible in the radial force balance (Smith and Montgomery 2008).

In contrast to the traditional evaluation of a model-simulated intensity using VMAX and PMIN, a complimentary evaluation of the structure of simulated tropical cyclones has emerged in the literature. Such an evaluation is often conveniently performed using the time–radius Hovmöller and/or the time-mean height–radius diagrams of azimuthally averaged tangential velocity and radial wind velocity (see, e.g., Smith et al. 2009; Wang 2009; Hill and Lackmann 2009; Xu and Wang 2010a,b; Fudeyasu and Wang 2011) of the vortex. The former is a diagnostic of the quasi-symmetric horizontal circulation and the latter is a diagnostic of the thermally direct vertical (transverse) circulation. These circulations are traditionally referred to as the ''primary circulation'' and ''secondary circulations,'' respectively, following, for example, Ooyama (1982). The combination of these two components gives rise to the picture of air parcels spiraling inward, upward, and outward.

Since the model-simulated radial inflow in the BL and above is driven by nonconservative processes (such as convection and surface friction) that tend to drive the flow away from the gradient-wind balance, an important question is how sensitive the PWR and the vortex structure simulated by a given tropical cyclone prediction model are to uncertainties in physics parameterization schemes. In particular, as the research and operational communities work together under the auspices of the National Oceanic and Atmospheric Administration's (NOAA) Hurricane Forecast Improvement

Project (HFIP; see http://www.hfip.org/)[1] to understand the degree to which a tropical cyclone intensity forecast can be improved in operational numerical weather prediction (NWP) models, it still remains a great challenge for the research community to reach a consensus on whether the current physics parameterizations in operational NWP models are suitable for a horizontal grid spacing of ≤3 km. To deal with these challenges, it is important to first understand how sensitive operational NWP models for hurricane forecasting are to different physics parameterizations, in terms of the standard PWR and vortex structure metrics discussed in the foregoing paragraph.

In this study, a series of idealized experiments with the NOAA Experimental Hurricane Weather Research and Forecasting Model (HWRFX) are performed for the purpose of evaluating the sensitivity of the HWRFX to commonly used BL and cloud microphysics parameterization schemes. The HWRFX is a version of the National Centers for Environmental Prediction's (NCEP) Hurricane Weather Research and Forecasting (HWRF) system specifically modified at the Hurricane Research Division (HRD) of the Atlantic Oceanographic and Meteorological Laboratory (AOML) and the Earth System Research Laboratory (ESRL) to study the intensity change problem at the finest model grid resolution operationally feasible at this time for forecasting. The model is initialized with a weak axisymmetric vortex disturbance in an idealized tropical environment that is favorable for the vortex amplification. The initial mass and wind fields associated with the weak vortex disturbance are obtained by solving the nonlinear balance equation for the given wind distributions of the initial vortex, and the prescribed background thermal profile. We employ the foregoing metrics, VMAX and PMIN, as well as the azimuthally averaged structure of the simulated tropical cyclone as away of quantifying the sensitivity of the intensification process to variations in physics parameterization schemes.

The remainder of the paper is organized as follows: the setup of the HWRFX sensitivity experiments is described in section 2. Our current understanding of the basic dynamics of tropical cyclone intensification is reviewed in section 3 to provide a meaningful context for the sensitivity experiments. The results from the various sensitivity experiments are presented and compared in

section 4. One of the outcomes of this section is the demonstration of the advantage of using the azimuthally averaged structural metrics over the VMAX and PMIN metrics used traditionally. A summary and discussion of the results are provided in section 5, along with their implications for tropical cyclone model evaluation.

2. Experimental design

The sensitivity experiments presented here are run with a parent domain (about 55° × 55°) at a horizontal resolution of 9 km with a single moving nest (about 8° × 8°) at 3-km horizontal resolution. There are 43 stretched pressure-sigma hybrid levels in the vertical direction with the top level set to 50 hPa.

To initialize the idealized vortex in all the experiments, the nonlinear balance equation in the pressure-based sigma coordinate system described in Wang (1995) is solved within the rotated latitude–longitude E-grid framework on an f plane located at 12.5°N. The mass field is derived from the wind field corresponding to an axisymmetric cyclonic vortex of maximum surface tangential wind set to 15 m s^{-1} at 90 km from the vortex center that is embedded in a quiescent flow. The temperature and humidity profiles of the far field are based on Jordan's Caribbean sounding (Jordan 1958; Gray et al. 1975). In all of the experiments, the sea surface temperature is set to 302 K (approximately 29°C).

The physics configurations used in all the sensitivity experiments are summarized in Table 1. One of these configurations (experiment 1) is very close to the operational HWRF system, in which the HWRF version of the Global Forecast System (GFS) surface and BL formulations are used to parameterize the sea-to-air flux transport and the subsequent mixing in the atmosphere. The Ferrier (FER) scheme is used to provide latent heating due to the microphysical processes of clouds in the atmosphere, and the Simplified Arakawa and Schubert (SAS) scheme (see Pan and Wu 1995) is used to parameterize subgrid-scale cumulus-cloud activity. The National Center for Atmospheric Research (NCAR) longwave and shortwave radiation schemes are used. To maintain consistency between our results at 9 and 3 km and those in Gopalakrishnan et al. (2011a), the SAS convection scheme is used at 3-km resolution along with the Ferrier scheme for grid-resolved cloud microphysics processes. Whether a subgrid convective parameterization (SCP) scheme should be turned on in the 3-km grid and, if so, whether the SAS scheme is an appropriate one to use, remain subjects of research. As shown by one of the sensitivity experiments in this study, turning on the SAS scheme in the 3-km grid basically modifies the latent heating distribution that is realized by the explicit microphysics scheme only and thus

---

TABLE 1. The suite of sensitivity experiments. Explanations of the individual physics options are available online (http://www.dtcenter.org/HurrWRF/users/docs/scientific_documents/HWRF_final_2-2_cm.pdf and http://www.dtcenter.org/HurrWRF/users/online_tutorial/tutorial02222010.php).

Experiment number and name (color symbol designation in the VMAX and PMIN time series shown in section 4)	Description of physics options
1 GFS/SAS/FER/NCAR (red)	GFS BL and surface scheme, SAS convective scheme on both grids, Ferrier microphysics scheme, NCAR Rapid Radiative Transfer Model longwave radiation scheme, Dudhia shortwave radiation scheme
2 MYJ/SAS/FER/NCAR (black)	MYJ BL and surface scheme, SAS convective scheme on both grids, Ferrier microphysics scheme, NCAR Rapid Radiative Transfer Model longwave radiation scheme, Dudhia shortwave radiation scheme
3 MYJ/BMJ/FER/NCAR (gray)	MYJ BL and surface scheme, Betts–Miller–Janjić convective scheme on both grids, Ferrier microphysics scheme, NCAR Rapid Radiative Transfer Model longwave radiation scheme, Dudhia shortwave radiation scheme
4 GFS/BMJ/FER/GFDL (orange)	GFS BL and surface scheme, Betts–Miller–Janjić convective scheme on both grids, Ferrier microphysics scheme, GFDL radiation scheme
5 GFS/BMJ/FER/NCAR (pink)	GFS BL and surface scheme, Betts–Miller–Janjić convective scheme on both grids, Ferrier microphysics scheme, NCAR Rapid Radiative Transfer Model longwave radiation scheme, Dudhia shortwave radiation scheme
6 GFS/SAS/FER/NCAR/MOD-DRAG (brown)	GFS BL and surface scheme, SAS convection scheme on both grids, Ferrier microphysics scheme, NCAR Rapid Radiative Transfer Model longwave radiation scheme, Dudhia shortwave radiation scheme, realistic drag coefficient consistent with recent observations
7 GFS/SAS/WSM5/GFDL (light blue)	GFS BL and surface scheme, SAS convection scheme on both grids, WRF single-moment 5-class microphysics scheme, GFDL radiation scheme
8 GFS/SAS/WSM6/GFDL (magenta)	GFS BL and surface scheme, SAS convection scheme on both grids, WRF single-moment 6-class microphysics scheme, GFDL radiation scheme
9 GFS/SAS/Thom/GFDL (yellow)	GFS BL and surface scheme, SAS convection scheme on both grids, WRF Thompson microphysics scheme, GFDL radiation scheme
10 GFS/SAS/FER/GFDL (green)	GFS BL and surface scheme, SAS convection scheme on both grids, Ferrier microphysics scheme, GFDL radiation scheme
11 GFS/noSAS/FER/GFDL (purple)	GFS BL and surface scheme, SAS convection scheme on 9-km grid, no convective scheme on 3-km grid, Ferrier microphysics scheme, GFDL radiation scheme

influences the intensity and structure of the simulated TC. The effect of radiation is investigated by changing the longwave and shortwave radiation schemes from the NCAR scheme to the Geophysical Fluid Dynamics Laboratory (GFDL) scheme.

The results from all the experiments listed in Table 1 are divided into three groups to allow for the examination of the sensitivity of the simulated tropical cyclone development (i) to BL mixing, subgrid convection, and radiation (experiments 1–5), (ii) to the surface drag (experiments 6 and 7), and (iii) to the bulk microphysics and subgrid convection schemes (experiments 8–11). The BL mixing schemes determine the vertical subgrid turbulence mixing and vertical diffusion within the atmospheric boundary layer and the free atmosphere above. The two schemes used in this study (i.e., the Mellor–Yamada–Janjić (referred to as MYJ) and the GFS BL schemes) are both one-dimensional and representative of two types of

BL mixing parameterizations widely used in numerical weather prediction models: the turbulent kinetic energy (TKE) scheme and the flux scaling scheme. The drag and enthalpy exchange coefficients used in the MYJ BL scheme are calculated using the surface layer scheme developed by Janjić (1996, 2002), and are based on the Monin–Obukhov similarity theory and include parameterizations of a viscous sublayer. In the GFS BL scheme, on the other hand, the drag and enthalpy exchange coefficients are calculated in a nearly identical way to the operational GFDL hurricane model, which is a bulk parameterization based on the Monin–Obukhov similarity theory. In both of the BL schemes, the drag and enthalpy exchange coefficients increase with 10-m wind speed. Two subgrid convection schemes are permutated in the experiments: the SAS scheme and the Betts–Miller–Janjić (BMJ) scheme (Janjić 1994, 2000). In addition to the NCAR longwave and

shortwave radiation schemes, the GFDL schemes for longwave and shortwave radiation are used in the sensitivity experiments. The surface drag coefficient calculation for the sensitivity experiments is described in section 4b.

A total of four different microphysics schemes are used in the sensitivity experiments: the Ferrier scheme, the WRF single-moment 5-class (WSM5) scheme, the WRF single-moment 6-class (WSM6) scheme, and the Thompson double-moment 6-class (Thom) scheme (Skamarock et al. 2008). The Ferrier scheme predicts changes in water vapor and condensate in the forms of cloud water, rain, cloud ice, and precipitation ice (snow/graupel/sleet) (see Skamarock et al. 2008). The individual hydrometeor fields are combined into total condensate for advection calculation. The WSM5 scheme has five prognostic equations of microphysical processes for vapor, rain, snow, cloud ice, and cloud water, and allows supercooled water to exist and a gradual melting of snow as it falls below the melting layer. The WSM6 scheme extends the WSM5 scheme to include graupel and its associated processes. The Thompson double-moment scheme includes six prognostic equations of moisture species plus the number concentration for ice as prognostic variables. Since only water vapor and total condensate are advected in the Ferrier scheme, the horizontal and vertical advection of hydrometeor species in all the non-Ferrier schemes are consistently treated in accordance with the assumptions made in the Ferrier scheme (i.e., keeping the partition of hydrometeors unchanged during the advection of the total condensate), such that the differences in all the microphysics schemes are kept in the parameterization of cloud microphysical processes.

3. Metrics for comparing the sensitivity experiments

To understand the salient characteristics of the model solution and improve the model performance, it is important to choose metrics that carry dynamical information for the examination of sensitivity experiments. The results from all the sensitivity experiments summarized in Table 1 will first be compared in terms of the intensity of the simulated tropical cyclone using VMAX, PMIN, and PWR. Then, the structures of the simulated tropical cyclone in the sensitivity experiments will be compared in terms of azimuthally averaged winds and acceleration. The latter metrics for comparison are necessary to complement the intensity comparison. This is because observations suggest that the intensity in terms of the VMAX and PMIN of tropical cyclones is not strongly correlated with its size (e.g., Weatherford and Gray

1988), and simply using the intensity metric to compare the sensitivity experiments is insufficient for providing useful information for understanding and improving the model performance. Thus, in this section, a brief review is provided to summarize the advantages and weaknesses of these metrics.

The intensity of tropical cyclones is operationally described in terms of minimum sea level pressure of the cyclone center (i.e., PMIN) and the local maximum surface wind speed (i.e., VMAX). The advantage of using PMIN in operational forecasts and climatological records is that it can be obtained reliably from dropsonde measurements or direct observations at an aircraft reconnaissance flight level. On the other hand, VMAX is a difficult quantity to measure by definition (i.e., 10-m level, 1 min sustained), despite the fact that it is often related to the destructive energy[2] and societal impact of tropical cyclones because of its close link to the structure of tropical cyclones. For this reason, pressure–wind relationships were developed to fulfill the need for describing tropical cyclone intensity in terms of VMAX in accordance with PMIN [for useful historical perspectives see Knaff and Zehr (2007) and Holland (2008)]. Although these PWRs were attempts to describe the mean relationship between PMIN and VMAX, the actual relationship between them is a function of multiple factors related to the tropical cyclone environment and structure that varies from case to case. Consequently, there is considerable scatter about any given PWR derived from observations [see, e.g., both Fig. 7 and Table 1 in Holland (2008) for a statistical summary]. This hinders the effectiveness of using the observationally derived PWRs to gain insight into the scattering of the PWRs from the sensitivity experiments, particularly when the sensitivity spread lies within the uncertainties associated with the observed PWR.

There is also a fundamental weakness in comparing the observationally derived PWRs to those from the sensitivity experiments. The development of the PWRs based on observations is, historically, motivated by the assumption that the gradient-wind balance is dominant in the overall dynamics of tropical cyclone intensification. Although the gradient-wind balance embedded in the observationally derived PWRs appears to contain all of the essential dynamics of the vortex tangential wind above the BL, it is fundamentally invalid in the BL. The gradient-wind balance is formally invalid in the BL because, first, it assumes that the radial inflow makes a negligible impact to

---

[2] Strictly speaking, the destructive energy of tropical cyclones is related to storm-integrated kinetic energy, which is closely linked to storm structure.

the dynamics there. This is not the case in the BLs of tropical cyclones [see, e.g., Montgomery et al. (2006) and also the scale analysis by Smith and Montgomery (2008) and Smith and Vogl (2009)]. Second, VMAX in the PWR is the locally, instantaneous maximum wind near the surface, while the wind required by the gradient-wind balance is axisymmetric. Thus, it seems inherently problematic to seek a physically meaningful understanding of the sensitivity experiments if only the model-simulated PWRs are compared.

On the other hand, since the gradient-wind balance is a good approximation to the azimuthally averaged dynamics above the BL (e.g., Bui et al. 2009 and references therein), it seems physically appropriate to use the azimuthally averaged structure of the simulated tropical cyclone to compare the sensitivity experiments. Examples of useful parameters for illustrating the cyclone structure are the azimuthally averaged radius of the 15 m s^{-1} [slightly less than the lower threshold of gale-force winds (17 m s^{-1})] and radius of the 35 m s^{-1} tangential velocity (slightly greater than the 33 m s^{-1} definition of hurricane strength). In fact, in some previous studies (e.g., Xu and Wang 2010a,b), the radius of the damaging-force [50 kt ($\sim$25.7 m s^{-1})] wind is used often as a size parameter of the simulated vortex.

Using the azimuthally averaged structure to compare the sensitivity experiments takes advantage of the current understanding of the dynamics of the primary and secondary circulations associated with an axisymmetric vortex. The essential premise of this understanding is that the primary circulation of a tropical cyclone vortex is so strong that the mean axisymmetric dynamics broadly control the dynamics of tropical cyclone intensification and structural evolution [see Willoughby 1995; Bui et al. 2009; and section 2 of Montgomery and Smith (2011, manuscript submitted to *Quart. J. Roy. Meteor. Soc.*, hereafter MOSM)]. These two spinup mechanisms have been identified to coexist during the intensification of the primary circulation (see section 7 of MOSM).

In the first spinup mechanism, the intensification of the primary circulation can be explained by the convergence driven by the aggregate diabatic heating in the eyewall region associated with the rotating deep convection and the material conservation of the absolute angular momentum. The secondary circulation of tropical cyclones can be understood dynamically as the response of a balanced axisymmetric vortex above to lateral and vertical forcing distributions associated with diabatic processes and their interaction with the environment and the lower boundary. Such a response can be described by diagnostic solutions of Eliassen's balanced vortex equations (see, e.g., Shapiro and Willoughby 1982, Bui et al. 2009; and section 2 of MOSM).

The surface forcing associated with the surface drag and the turbulent sensible and latent heat fluxes can further distort the primary and secondary circulations that intensify with this spinup mechanism, as seen in work of Willoughby (1979), Schubert and Hack (1982), Shapiro and Willoughby (1982), and Bui et al. (2009).

The second spinup mechanism is associated with the intensification of the primary and secondary circulations within the BL. It requires that the radial pressure gradient increases with time, which, in turn, requires spinup of the tangential wind at the top of the BL by the first mechanism. This mechanism becomes progressively important in the eyewall region as the vortex intensifies. During the intensification, although absolute angular momentum is not conserved in the BL, the largest wind speeds anywhere in the vortex can be achieved in the boundary layer. This occurs when the radial inflow is sufficiently large to move air parcels close to the vortex center without a large loss of absolute angular momentum. This mechanism is coupled to the first one through BL dynamics because the radial pressure gradient of the BL is determined by the overall vortex flow above the BL as discussed in section 2.6 of MOSM. This spinup mechanism explains why the maximum azimuthally averaged tangential wind speeds in the model simulations (e.g., Smith et al. 2009) are located near the top of the boundary layer.

The major caveat of using other metrics such as those proposed in the foregoing discussion for comparing the sensitivity experiments is that it requires more observational information about the azimuthally averaged structure of real tropical cyclones (e.g., see Rogers et al. 2012, Gopalakrishnan et al. 2011b) to help discriminate which of the sensitivity experiments is more realistic. Although general structural information about tropical cyclones has been reasonably well documented now (e.g., Houze 2010), information about the structure of individual tropical cyclones is not as readily available as estimates of VMAX and PMIN. However, information on historical tropical cyclone events derived from aircraft observations is available at AOML/HRD to provide the needed structural evaluation of the HWRFX simulations in future studies.

4. Results

In this section, we focus on the results from the sensitivity experiments for the idealized tropical cyclone intensification scenario. The results of the sensitivity experiments are compared in terms of time series of the minimum mean sea level pressure at the center of the cyclone, the spatially local maximum 10-m wind speeds around the center, and the PWR from the 3-km grid.

The structures of the simulated tropical cyclone from the sensitivity experiments are compared also in terms of the axisymmetric mean primary and secondary circulations created from hourly model output for the entire period of the simulation.

a. Sensitivity to boundary layer mixing, subgrid convection, and radiation (experiments 1–5)

During intensification, the enthalpy from the sea surface driven by thermal disequilibrium across the air–sea interface is transported upward and consumed by the tropical cyclone. Such transport is accomplished primarily by turbulence- and convection-induced vertical mixing processes in the BL. In light of these, the first set of five sensitivity experiments (experiments 1–5 in Table 1) is used to reveal the dependency of the HWRFX-simulated tropical cyclone intensification on the choice of BL mixing, subgrid convection, and radiation parameterization schemes. Figure 1 depicts the time series of PMIN and VMAX from these experiments. The time series indicates the relative sensitivity of the simulated intensification to variation in the BL scheme (experiments 1 and 2), the subgrid convective scheme (experiments 1 and 5, 2 and 3), and the radiation scheme (experiments 4 and 5).

Figure 1 shows that experiments 1 and 2, which differ only in BL schemes, have similar development trends in the spinup stage of the first 36 h. However, after 36 h, the simulation with the GFS scheme persistently produces a greater VMAX than the simulation using the MYJ scheme. Although the differences between the two schemes are not only in the formulations of the vertical diffusion but also in the details of how the surface momentum and enthalpy flux are calculated, a separate study (J.-W. Bao et al. 2011, unpublished manuscript) has shown that the differences in the intensity are more associated with the differences in the surface flux calculation, while the differences in the structure are more associated with the differences in the vertical diffusion. Figure 1 shows also that the differences in the subgrid convection scheme produce more differences in the simulated tropical cyclone intensification than the differences in the BL schemes (see the differences between experiments 1 and 5 versus experiments 1 and 2, or experiments 2 and 3 versus experiments 1 and 2). Also, when the BMJ convective parameterization scheme is used, the tropical cyclone develops much more slowly than when the SAS scheme is used, although both simulations reach similar intensities toward the end of the simulations. The differences made by the two different radiation schemes (experiments 4 and 5) are the smallest among the five experiments. It is interesting to note in Fig. 1 that because of the differences
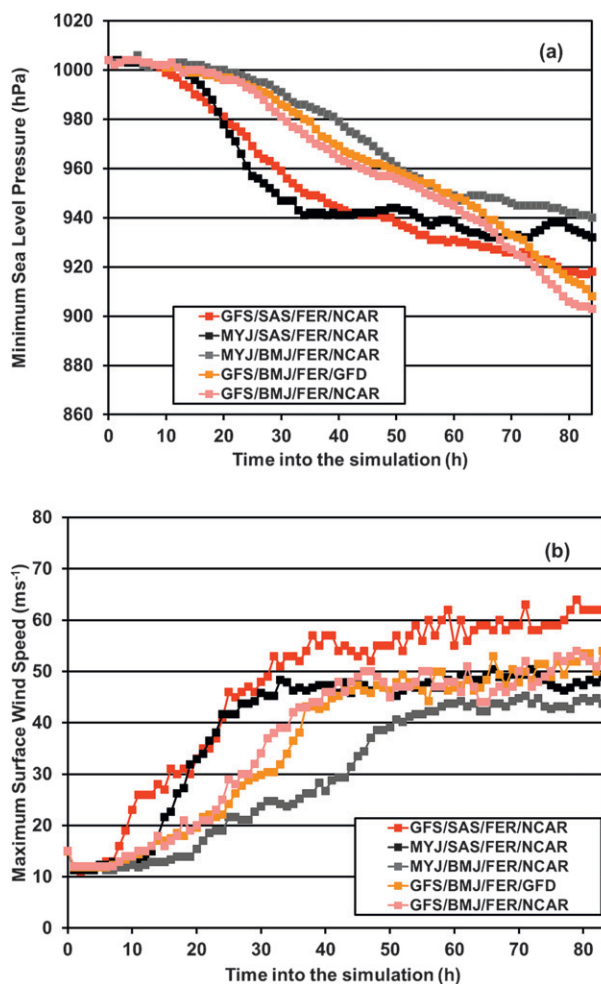

FIG. 1. (a) Min sea level pressure (hPa). (b) Max surface wind speed (m s^{-1}). The red lines are expt 1 (GFS/SAS/FER/NCAR schemes), the black lines are expt 2 (MYJ/SAS/FER/NCAR schemes), the gray lines are expt 3 (MYJ/BMJ/FER/NCAR schemes), the orange lines are expt 4 (GFS/BMJ/FER/GFDL schemes), and the pink lines are expt 5 (GFS/BMJ/FER/NCAR schemes).

in the inner-core size of the simulated tropical cyclone (defined as RMW), the intensity looks more similar in terms of PMIN than VMAX.

It is important to recognize that the two different BL schemes produce a significant difference in the asymptotic behavior of PMIN. Figure 1 shows that VMAX from all five experiments levels off and becomes quasi-steady after 60 h into the simulation. While PMIN from all the experiments continues to decrease after 60 h, the decrease slows down in the two experiments using the MYJ BL scheme, but remains almost the same in all the experiments using the GFS BL scheme. It is expected that for a steady environment such as the one prescribed in all the experiments herein, the simulated cyclone should eventually reach a quasi-steady state in which

the inner-core size and intensity of the simulated cyclone undulate with small amplitudes[3] and the overall intensification of the simulated cyclone ceases.

Since the major difference in the asymptotic behavior of PMIN shown in Fig. 1 occurs with the different BL schemes, this would suggest that the BL scheme plays an important role in determining how the simulated cyclone reaches the quasi-steady state. It is obvious that the experiments using the GFS BL scheme takes longer to approach a quasi-steady state than those using the MYJ BL scheme. The implication of this particular result for the evaluation of hurricane prediction models is believed to be nontrivial since it is unknown in theory how long it takes for a weak initial vortex, such as the one used in this study, to reach the quasi-steady state corresponding to the prescribed environment. It is also unknown what primary structural characteristics (e.g., spatial distributions of wind and thermal properties) the quasi-steady cyclone should have. These considerations suggest that other metrics are necessary to evaluate the behavior of the HWRF model with changes in physics, particularly when PMIN continues to decrease with time while VMAX becomes quasi-steady.

Figure 2 compares the five experiments in terms of the PWR. Until VMAX > 55 m s^{-1} and PMIN $<$ 940 hPa, experiment 1 produces a correspondence in the trend of VMAX and PMIN that is close to the statistical mean obtained by Knaff and Zehr (2007) and within the spread of uncertainty (see more discussion below). The two experiments with a different subgrid convection scheme (experiment 5) and a different radiation scheme (experiment 4) than the ones used in experiment 1 produce similar correspondences in the trend of VMAX and PMIN until VMAX $>$ 50 m s^{-1} and PMIN $<$ 950 hPa. The use of the MYJ BL scheme (experiments 2 and 3) leads to a significantly different trend of PWR than in experiment 1. Overall, the MYJ scheme tends to produce a smaller VMAX for a given PMIN than the GFS scheme. More data points from the experiments using the MYJ scheme for VMAX greater than 40 m s^{-1} and PMIN lower than 940 hPa are clustered together than those from the experiments using the GFS BL scheme. This clustering is a manifestation of the fact that the simulated cyclone in the experiments using the MYJ scheme
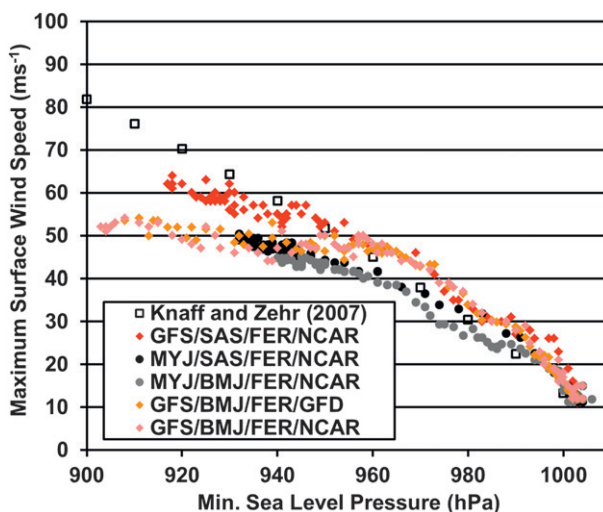
---

[3] Such undulation is associated with replenishment cycles of the primary eyewall in which the inner-core structure of the simulated vortex undergoes rapid changes due to the development of outer rainbands and their ensuing coalescence into the existing primary eyewall, and/or the formation of a secondary outer eyewall that sequentially undergoes contraction and replaces the primary eyewall.

FIG. 2. Min sea level pressure (hPa) vs max surface wind speed (m s^{-1}). The red filled diamonds are expt 1, the black filled circles are expt 2, the gray filled circles are expt 3, the orange filled diamonds are expt 4, the pink filled diamonds are expt 5, and the open squares are from Knaff and Zehr (2007). The open red triangles (expt 1) and the open black circles (expt 2) are the min sea level pressure (hPa) vs the surface max azimuthally averaged tangential wind speed.

approaches the quasi-steady state faster than that from the experiments using the GFS BL scheme.

It should be pointed out that caution needs to be applied when comparing the model-simulated PWRs with the statistical mean, such as the one obtained by Knaff and Zehr (2007). First, the datasets used in the derivation of the PWRs have uncertainty. Knaff and Zehr (2007) and Holland (2008) pointed out that the datasets used to produce the various statistical mean PWRs have large scatter. For example, careful examination of Fig. A1 in Knaff and Zehr (2007) and Fig. 7 in Holland (2008) reveals that, for VMAX > 40 m s^{-1}, the scatter about the mean is as large as 10 m s^{-1}. It is seen from our Fig. 2 that the largest differences in VMAX are caused by the differences in the BL parameterization schemes, which are within the magnitude of about 10 m s^{-1} and comparable with the uncertainty in the datasets used in the derivation of the statistical PWRs. Second, there is a discrepancy between the model output sampling and observational data sampling when defining VMAX. VMAX from the model is defined as instantaneous maximum 10-m wind at the beginning of each hour of the simulation. While by definition the observed VMAX is the maximum 10-m, 1-minute sustained wind, there is a quite large disparity in data sampling with different instrumentation techniques. Third, the gradient-wind balance is applied as a guide in the derivation of the statistical mean PWRs [see more

detailed discussion of this in Knaff and Zehr (2007)]; however, as discussed earlier, such a balance is not valid in the BL near the surface where the mean radial inflow is no longer negligible in mature tropical cyclones, as is required in the gradient balance approximation (Smith and Montgomery 2008). In fact, when the surface maximum azimuthally averaged tangential winds are compared with the statistical mean PWR in Fig. 2, the differences between the experiments with the GFS (open red triangles in Fig. 2) and MYJ (open black circles in Fig. 2) BL schemes are much smaller than those shown by VMAX. This strongly suggests that any PWR-based metric for comparing results from physics sensitivity experiments is inadequate to reveal physically meaningful information in a conclusive manner.[4] It suggests also that PMIN and VMAX are less dynamically coupled for VMAX > 50 m s^{-1} than for smaller VMAX. Therefore, it is necessary to use other metrics to compare the sensitivity experiments. In fact, we will demonstrate below that structural metrics such as Hovmöller diagrams of the maximum azimuthally averaged tangential wind speed are better than VMAX and PMIN for revealing the differences in the sensitivity experiments.

The sensitivity of the simulated cyclone intensity to various BL, subgrid convection, and radiation schemes, as revealed in Figs. 1, 2, is also associated with changes in the structure of the simulated tropical cyclone. As illustrated in Liu et al. (1999), Zhang et al. (2001), Smith et al. (2009), and Gopalakrishnan et al. (2011a), it is convenient and helpful to examine the structure of model-simulated tropical cyclones in terms of the axisymmetric mean circulations in the cylindrical coordinate (r, λ, z) system, where r is the distance from the center of the vortex, λ is the azimuthal angle, and z is the vertical height. Such an analysis has been shown to be quite illuminating in observational analyses also (e.g., Marks et al. 1992). To facilitate the analysis of the

model output from the sensitivity experiments in the cylindrical coordinate system, the horizontal equations of motion in the HWRFX are transformed into radial and tangential momentum components:

$$\frac{du_r}{dt} = -\frac{1}{\rho}\frac{\partial p}{\partial r} + \frac{v_\lambda v_\lambda}{r} + f v_\lambda + D_{ur}, \quad (1)$$

$$\frac{dv_\lambda}{dt} = -\frac{1}{\rho r}\frac{\partial p}{\partial \lambda} - \frac{u_r v_\lambda}{r} - f u_r + D_{v\lambda}, \quad (2)$$

where $d/dt = \partial/\partial t + u_r(\partial/\partial r) + (v_\lambda/r)(\partial/\partial \lambda) + w(\partial/\partial z)$ is the material derivative operator in which u_r, v_λ, and w are, respectively, the radial, tangential, and vertical velocities in the earth-relative transformed coordinate system. Also, p is the pressure, f is the Coriolis parameter, and D_{ur} and $D_{v\lambda}$ are, respectively, the diffusion (frictional) terms in the radial and tangential directions. In the absence of surface friction and the terms that constitute the radial wind acceleration, (1) reduces to the gradient-wind balance equation, while (2) represents the material acceleration of the tangential velocity and the material conservation of absolute angular momentum (see section 2.4 in MOSM).

Figure 3 shows the Hovmöller diagrams of the azimuthally averaged instantaneous tangential wind speed at 1 km above the model sea surface and at hourly outputs from 0 to 84 h into the simulations. The structure at 1 km was chosen to minimize the effects of friction. The most prominent sensitivity feature shown in Fig. 3 is the differences in the azimuthally averaged maximum tangential wind speed and the radius of the 35 m s^{-1} contour. These results indicate also that the structure of the HWRFX-simulated tropical cyclone is more sensitive to changes in either the BL scheme or the subgrid convection scheme than the radiation scheme. Particularly, the MYJ BL scheme produces a more compact simulated cyclone with stronger 1-km tangential winds than the GFS BL scheme (note that this is opposite to what is seen with the surface winds), and the BMJ subgrid convection scheme produces slower intensification than the SAS convection scheme. The overall size of the simulated cyclone characterized by 35 m s^{-1} radii in all the experiments increases with time, but the rate of increase is more sensitive to the choice of BL scheme than either the subgrid convection or the radiation scheme. The MYJ BL scheme leads to a smaller inner-core size increase with time than the GFS BL scheme. The reason for this difference is the fact that the MYJ BL scheme produces smaller vertical eddy diffusivity than the GFS BL scheme does, and the detailed causality will be explored in a subsequent paper.

---

[4] It is worth mentioning that although the gradient-wind balance was used as a guide to derive the statistical PWR, the actual statistical PWR is not completely constrained by the gradient-wind balance because of the statistical regression. Consequently, the statistical PWR may represent some of the overall dynamical relation between the mass and wind fields in TC vortices above the BL that is different from the gradient balance approximation. Such a dynamical relation may include other information beyond VMAX and PMIN, such as the vortex size and the intensity tendency as a function of environment and geographical location. While it is still unclear what this additional information entails physically and mathematically, to a certain degree the statistical PWR may be regarded as the best fit to the "observed" actual relation between the hurricane mass and wind fields. Therefore, it is still useful to use it for model evaluation.
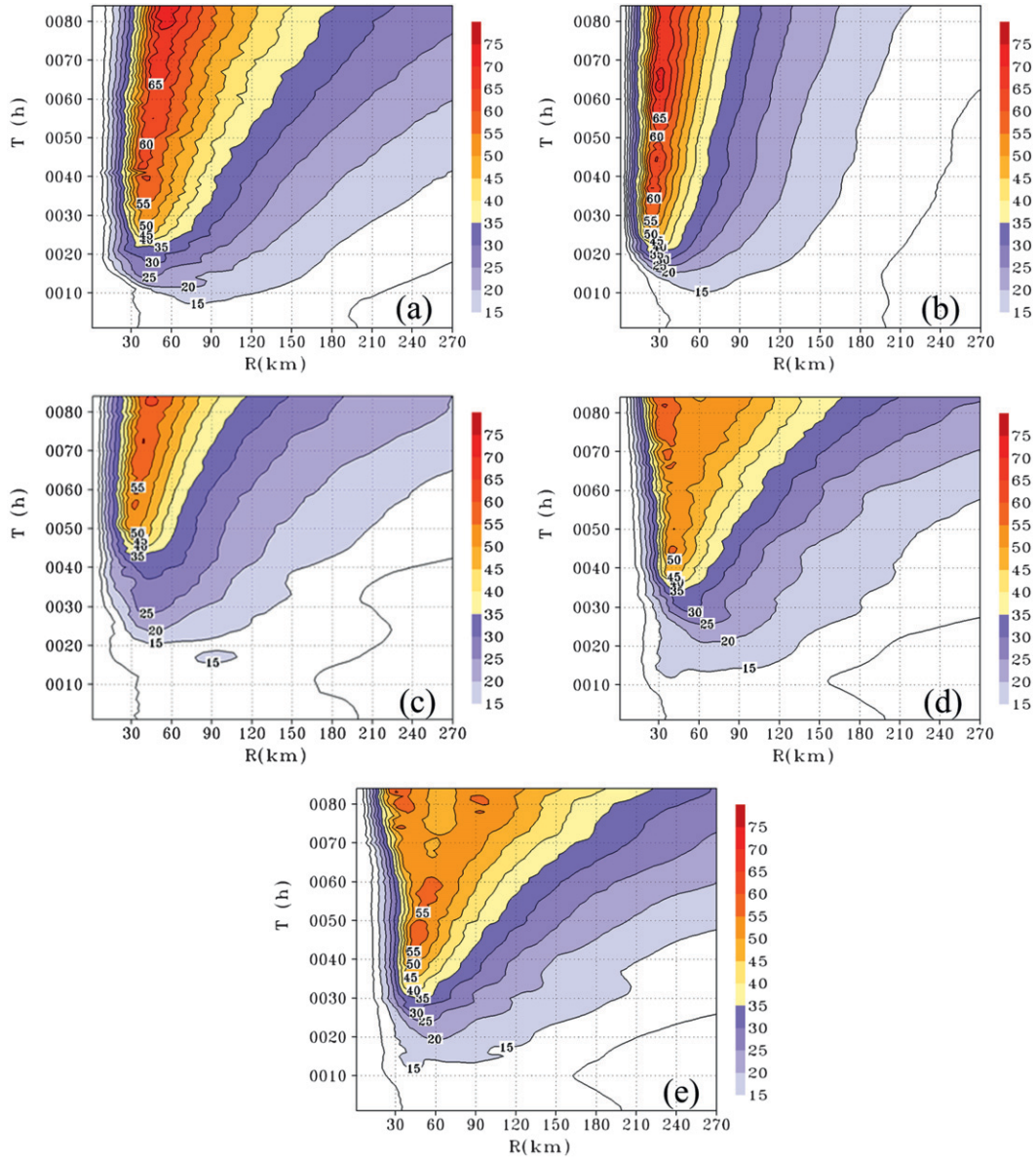
FIG. 3. Hovmöller diagrams of the azimuthally averaged tangential wind speed (m s^{-1}) for (a) expt 1, (b) expt 2, (c) expt 3, (d) expt 4, and (e) expt 5 at 1 km above the surface. The shaded and contour intervals are 5 m s^{-1}.

Figure 3 is a good example for showing the advantage of structure metrics such as the Hovmöller diagram in shedding light on the comparisons of the intensity in terms of VMAX and PMIN. In fact, Fig. 3 suggests a close connection between the inner-core size increase and the departure of the simulated VMAX–PMIN relation from the statistical one for PMIN < 940 hPa. This example also illustrates one of the problems in tropical cyclone model evaluation using only VMAX to represent the overall intensity of the simulated tropical cyclone. Despite these Hovmöller diagrams showing that the cyclone intensity in terms of the maximum wind

speed at 1 km above the model sea level in the experiment using the MYJ BL scheme is greater than that in the run using the GFS BL scheme, the corresponding VMAX shown in Fig. 1 (defined as the local peak 10-m wind around the center of the cyclone) is smaller.

Figure 4 depicts the azimuthally and 12-h averaged radius–height cross sections of the tangential wind contours superimposed on the vectors of the secondary circulation, contours of the radial wind speed, and the material acceleration in the tangential direction as described by (2), with the friction effect included for all five experiments. The time averaging is done over
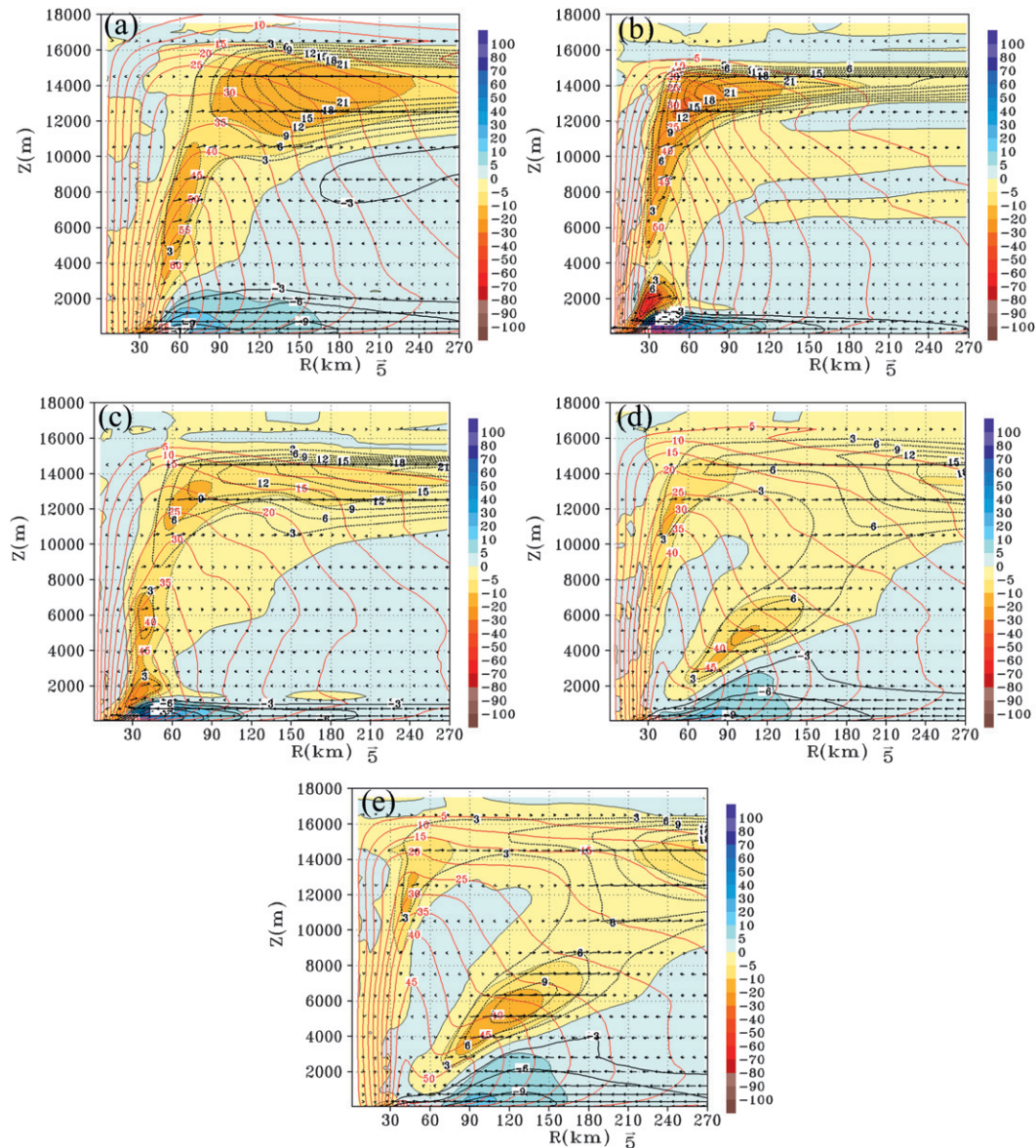
FIG. 4. Azimuthally and 60–72-h averaged radius–height cross sections of the tangential wind contours (in red) superposed on the secondary circulation vectors, radial wind speed (black contours; m s^{-1}), and the net tangential forcing (frictional effect included) in units of m s^{-1} h^{-1} (color shaded) related to the primary circulation term in (2) for (a) expt 1, (b) expt 2, (c) expt 3, (d) expt 4, and (e) expt 5. The positive contribution toward the spinup process is indicated by the blue end of the spectrum.

60–72 h, representing the quasi-steady stage of the simulated VMAX, and is required to better represent the quasi-steady state by reducing the small temporal undulations in the simulated structure. The intensity of the tangential circulation following the area enclosed by the 30 and 50 m s^{-1} red contours, as well as the tangential material acceleration, varies with the choices of BL. The MYJ BL scheme results in a greater maximum tangential wind speed and material acceleration in the eyewall region than the GFS BL scheme (cf. Fig. 4a with

4b and Fig. 4c with 4e), but smaller areas enclosed by the 30 and 50 m s^{-1} contours. That is, the MYJ BL scheme tends to produce a stronger but smaller vortex than the GFS BL scheme. Additionally, the radius of the maximum tangential wind speed above the low-level inflow is smaller in the experiments with the MYJ BL scheme than in the experiments with the GFS BL scheme. However, the near-surface tangential winds in the experiments with the MYJ BL scheme are weaker than in the experiments with the GFS BL scheme, which is

consistent with what is shown in Fig. 1 where the 10-m winds are weaker with the MYJ BL than with the GFS BL scheme. This result clearly indicates that the MYJ BL scheme produces a greater vertical shear of tangential winds than the GFS BL scheme. Furthermore, the combination of the MYJ BL scheme and the BMJ subgrid convection scheme produces the weakest near-surface tangential winds because this combination produces an overall weaker storm, which is also consistent with Fig. 1. On the basis of these results, it is evident that the largest differences in the tangential winds in all five experiments are, to a great degree, restricted to the inner core.

As for the sensitivity of the simulated secondary circulation, Fig. 4 indicates that when the SAS convection scheme is used, the GFS BL scheme (experiments 1, 4, and 5) produces a deeper inflow layer than the MYJ scheme (experiments 2 and 3). The return flow above the inflow in the eyewall region in the simulation with the GFS BL scheme is also weaker than that in the simulation with the MYJ BL scheme. While the GFS BL scheme produces a stronger and deeper upper-level outflow than the MYJ BL scheme (experiments 1 and 2), the MYJ BL scheme produces a narrower eyewall, indicating stronger vertical motion above the low-level inflow than the GFS BL scheme. Comparing experiment 1 with experiment 5 indicates that the SAS subgrid convection scheme leads to a more vertical eyewall than the BMJ scheme, while the comparisons of experiments 1 and 5, along with experiments 2 and 3, show that the BMJ scheme produces a weaker secondary circulation corresponding to a slower intensification process as seen in the Hovmöller diagrams. It should be pointed out that the sensitivity shown thus far in Figs. 3, 4 reflects the fact that various combinations of the subgrid and BL mixing schemes lead to different 3D diabatic heating distributions associated with the formation and replacement cycles of primary circulations and the interaction between the primary circulation and the outer rainbands. The physical mechanism connecting the variation in the 3D diabatic heating distribution with the variation in the simulated TC intensity and structure has been revealed and documented in a series of studies by Wang (2009), Hill and Lackmann (2009), Xu and Wang (2010a,b), and Fudeyasu and Wang (2011).

Despite the foregoing demonstrated sensitivity of the intensity and structure of the simulated tropical cyclone to various BL schemes, the reasons behind the variations have yet to be determined. There are two possible factors contributing to the differences. First, it should be kept in mind that the differences in the BL schemes are not only in the formulations of the vertical diffusion but also in the parameterizations used in the surface momentum and enthalpy flux calculations. Second, the overall dynamical response of the numerical model varies with different realizations of subgrid turbulent mixing in the model, particularly in the BL inflow layer above the surface (see, e.g., Kepert 2012; S. G. Gopalakrishnan et al. 2012, unpublished manuscript). In fact, it is demonstrated in a separate study (J.-W. Bao et al. 2011, unpublished manuscript) that the differences in the intensity as shown above are more associated with the differences in the surface flux calculation, while the differences in the structure are more associated with the differences in the vertical diffusion. It is also shown in this separate study that the use of horizontal diffusion and the divergence damping term in the dynamical solver of the model, which possesses a degree of numerical artifact, contributes significantly to the sensitivity of the model solution to various BL schemes, particularly in terms of the inner-core size and the simulated PWR when VMAX become quasi-steady.

The sensitivity of the model solution to various physics representations can also be seen in the simulated inflow in the mid–upper troposphere between 4 and 8 km in Fig. 4. The sensitivity to the radiation scheme may be due to the cloud–radiation feedback to the total diabatic heating distribution as discussed in Fovell et al. (2010). It appears from Fig. 4 that the mid–upper-tropospheric weak inflow is more sensitive to the BL schemes (experiments 1 and 2) and the subgrid convection schemes (experiments 1 and 5) than the radiation schemes (experiments 4 and 5). When the MYJ BL scheme is used, the sensitivity to the subgrid convection schemes is not as great as when the GFS BL scheme is used. Several axisymmetric model studies (e.g., Ooyama 1982; Willoughby 1979; Yamasaki 1977) have illustrated the importance of this midlevel inflow layer to the slow evolution of a tropical cyclone vortex. Ooyama (1982) pointed out that the deep-layer inflow is, in essence, all that is needed for the intensification of cyclonic rotation because at that level surface friction is not affecting the evolution process. Willoughby (1979) pointed out that the development of this weak midlevel inflow may be related to inner-core warming. Recently, Fudeyasu and Wang (2011) pointed out that the midlevel inflow often develops in response to diabatic heating in outer rainbands and affects the size of the simulated TC. In the perspective of the two-mechanism spinup processes (MOSM), this inflow may enhance the convergence of angular momentum above the BL. However, despite the sensitivity of the mid–upper tropospheric weak inflow to various BL schemes, the time series of VMAX and PMIN are apparently most sensitive to the differences in the subgrid convection schemes.

It is shown (Figs. 4b,c) that the strong BL inflow associated with the MYJ BL scheme results in strong tangential acceleration near the surface, despite the effects

of friction that act to oppose the acceleration in the tangential direction. It is also worth pointing out that the MYJ BL scheme produces the strongest tangential winds in the inner core of the cyclone right above the maximum inflow, regardless of what subgrid convection scheme is used. Moreover, although the MYJ BL scheme generates a smaller radius of the maximum tangential winds than the GFS BL scheme, the intensity of the cyclone measured by VMAX shown in Fig. 1, defined as local maximum 10-m wind, indicates that the GFS BL scheme tends to produce a stronger mature cyclone. These results, on the one hand, are consistent with previous intensity-forecast studies using numerical weather prediction models (see, e.g., Braun and Tao 2000), which show a strong sensitivity of the model forecast to BL parameterization schemes. On the other hand, these results strongly suggest that in addition to VMAX and PMIN, which are conventionally used for model evaluation, observations of tropical cyclone structure (in terms of parameters such as the radii of the gale-force wind speed and the hurricane-force wind) together with the knowledge of the radius of the maximum tangential winds should be used in model evaluation and validation.

b. Sensitivity to surface drag (experiment 6)

This section focuses on the sensitivity of the idealized tropical cyclone intensification to changes in the surface drag coefficient. Some of the previous theoretical and numerical studies of the sensitivity to the surface exchange coefficients in axisymmetric models found that the intensity decreases markedly with increasing drag coefficient (e.g., Emanuel 1995; Craig and Gray 1996). In contrast, whereas a vortex intensifies in an axisymmetric model when there is no surface drag (see, e.g., Craig and Gray 1996), Montgomery et al. (2010) showed that no vortex intensification occurs in a three-dimensional model with zero surface drag (despite persistent sea-to-air fluxes of moisture to maintain deep convective activity). They showed also that the intensification rate and maximum intensity of the three-dimensional vortex increase with the increasing surface drag coefficient until a certain threshold value is attained and then the intensification rate decreases.

In both the GFS and MYJ BL schemes, the drag coefficient exhibits a steady increase with wind speed following the use of the Charnock formulation in the determination of the surface roughness from the momentum flux. Unfortunately, this wind speed dependency has not been corroborated by any observations for the marine boundary layer in the extreme wind conditions of tropical cyclones. Recent observations of Powell et al. (2003), Donelan et al. (2004), French et al. (2007), and
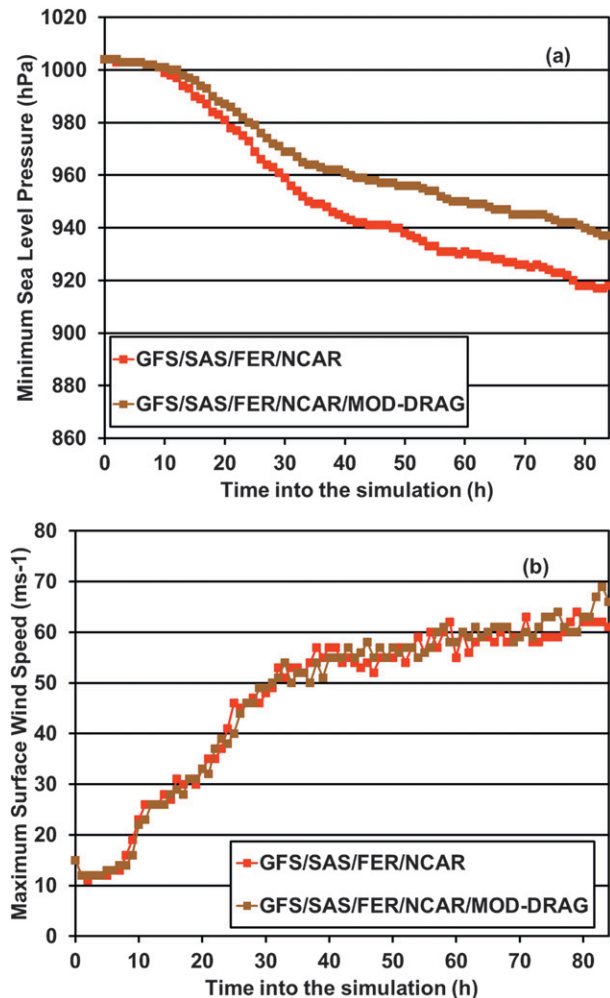

FIG. 5. (a) Min sea level pressure (hPa). (b) Max surface wind speed (m s^{-1}). The red lines are expt 1 and the brown lines are expt 6 (GFS/SAS/FER/NCAR/MOD-DRAG schemes).

Black et al. (2007) show that the drag coefficient exhibits a steady increase to a wind speed of approximately 30 m s^{-1} and then levels off for higher winds. To see how this behavior of the drag coefficient affects the cyclone intensification, experiment 6 is carried out, in which a realistic wind dependency of the drag coefficient is specified in the GFS BL scheme. In this experiment, since the exchange coefficient required for the determination of the surface sensible and latent heat fluxes is dependent on the drag coefficient, the impact the modified drag (MOD-DRAG) coefficient has on the surface sensible and latent heat fluxes is accounted for automatically in the surface flux calculation in the GFS BL scheme such that the heat exchange coefficient levels off at about 30 m s^{-1}.

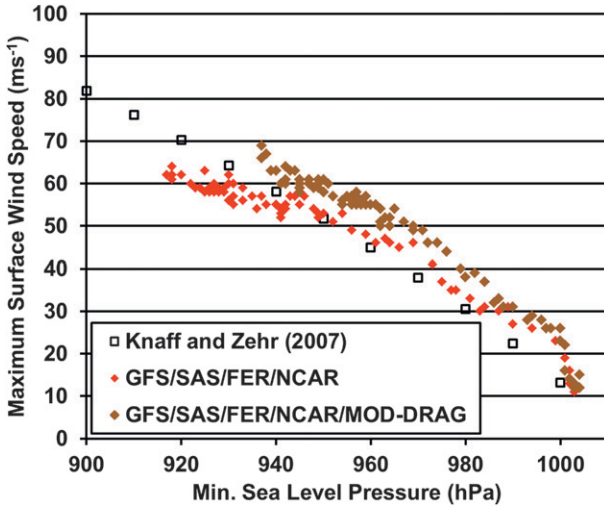Time series of PMIN and VMAX from experiment 6 are shown in Fig. 5 in comparison with those from

FIG. 6. Min sea level pressure vs max surface wind speed. The red filled diamonds are expt 1, the brown filled diamonds are expt 6, and the open squares are from Knaff and Zehr (2007).

FIG. 7. As in Fig. 3, but for expt 6.

experiment 1. In general, the modified drag coefficient produces a very similar intensification rate of the simulated tropical cyclone in terms of VMAX to the original one in the GFS BL scheme when VMAX exceeds 30 m s^{-1}. Although the decreasing rate of PMIN with the modified drag coefficient is smaller in experiment 6 than that in experiment 1, the PWR from experiment 6 (depicted in Fig. 6) exhibits a significantly different trend than that from experiment 1. It shows that the realistic wind dependency of the modified drag coefficient improves the PWR, indicating strongly that the surface drag coefficient is a key parameter in controlling the PWR in HWRFX when the GFS BL scheme is used. Overall, the differences made by the change in the drag coefficient are within the uncertainty of about 10 m s^{-1} in the Knaff and Zehr (2007) PWR, but the slope of the PWR is greatly improved for PMIN $<$ 970 hPa. This result is consistent with the role that the surface friction plays in disrupting gradient-wind balance and the conservation of angular momentum in the BL and, thus, is strongly related to the fact that smaller surface friction (associated with a more realistic surface drag coefficient in our case) lessens the disruption of the gradient-wind balance in the BL.

The use of the realistic wind dependency of the surface exchange coefficients also makes noticeable differences in the structure of the cyclone that are shown in the Hovmöller diagrams of the azimuthally averaged tangential wind speed at 1 km above the surface for experiment 6 (Fig. 7). Comparing Fig. 7 with 3a, the prominent differences made by the realistic wind dependency of the surface exchange coefficients are in the structure of the eyewall that is characterized by the
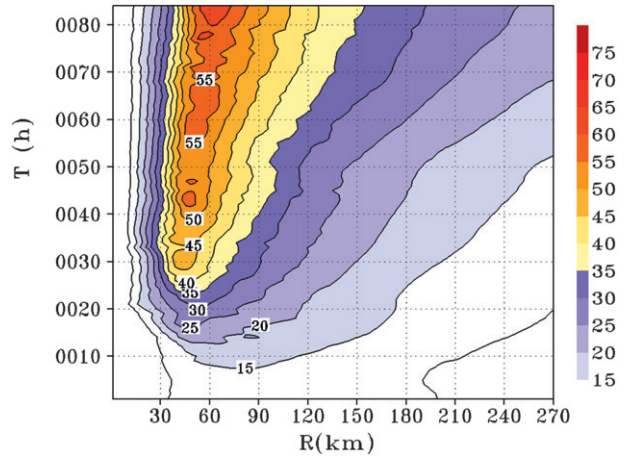
RMW and the 35 m s^{-1} contour. Overall, when the surface drag coefficient is modified to follow the observed wind dependency, the tangential winds within the eyewall become weaker and the reduced winds are accompanied by a decrease in the gradient force associated with surface friction during spinup. Figure 8 shows the azimuthally averaged radius–height cross section of the tangential wind contours superimposed on the vectors of the secondary circulation from experiment 6 (average between 60 and 72 h); shown also are the radial wind speed and the net forcing in the tangential direction. Comparing this cross section with those for experiment 1 shown in Fig. 4a, it is seen that the modified surface drag coefficient results in a decrease in the low-level acceleration of the tangential wind in the eyewall region above the boundary layer inflow, as well as a decrease in the intensity and depth of boundary layer inflow in the eyewall region. It can also be seen that as the surface drag increases, the RMW and the slope of the eyewall near the sea surface increase.
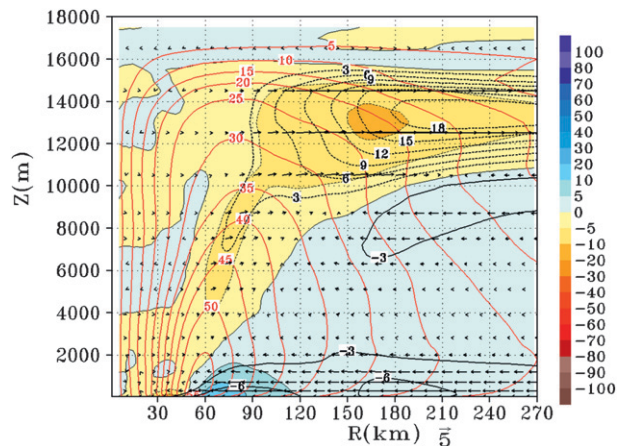

FIG. 8. As in Fig. 4, but for expt 6.

As discussed in the introduction, the spinup of the primary circulation is caused by the radial convergence of absolute angular momentum both above and in the (frictional) boundary layer. In the former case, the absolute angular momentum is approximately conserved materially, while in the latter it is reduced as air parcels spiral inward in the boundary layer on account of surface drag. Although it is recognized that the aggregate heating produced by the convection in the inner core is the primary forcing responsible for the radial convergence of absolute angular momentum above the boundary layer inflow, it does not seem possible for us to provide a simple link between the surface heat fluxes and the local cloud buoyancy necessary to support a deep overturning circulation. Nevertheless, as a step toward a more complete understanding, the significant change in the maximum tangential wind speed shown in Fig. 8 ($\sim$10 m s^{-1}) between the surface drag and the control experiments is found to be associated with a reduction in the radial convergence of angular momentum (both in and above the boundary layer) due to the decreased convection in terms of the grid-resolved vertical flux of water vapor in the eyewall region (not shown). The decreased convection is related in part to the decrease in the surface enthalpy flux associated with the decreased surface drag in the eyewall region.

c. Sensitivity to microphysics and subgrid convection schemes (experiments 7–11)

It has long been accepted that the primary energy source for the development and maintenance of a tropical cyclone is the latent heat that is transferred from the sea surface through the turbulent flux of water vapor and later released by condensation in convective clouds (MOSM and references therein). The structural evolution of the simulated tropical cyclone is also found to be sensitive to the details of the treatment of microphysics processes [see, e.g., Lord et al. (1984) for the effects of cloud ice and Smith et al. (2009) for the effects of the warm rain process]. As there has been a trend for tropical cyclone modelers to run numerical weather prediction models with higher spatial resolution using cloud microphysics schemes for describing convective clouds (either combining or dispensing with subgrid convection schemes), an immediate question to address is how sensitive the model-simulated intensification and structural evolution are to the differences in the details of cloud microphysics schemes and subgrid convection. Therefore, five more experiments (experiments 7–11) are carried out and analyzed to explore this question.

Figure 9 shows the time series of PMIN and VMAX from the five experiments (in comparison with those from experiment 1). Inspecting Fig. 9 reveals that the
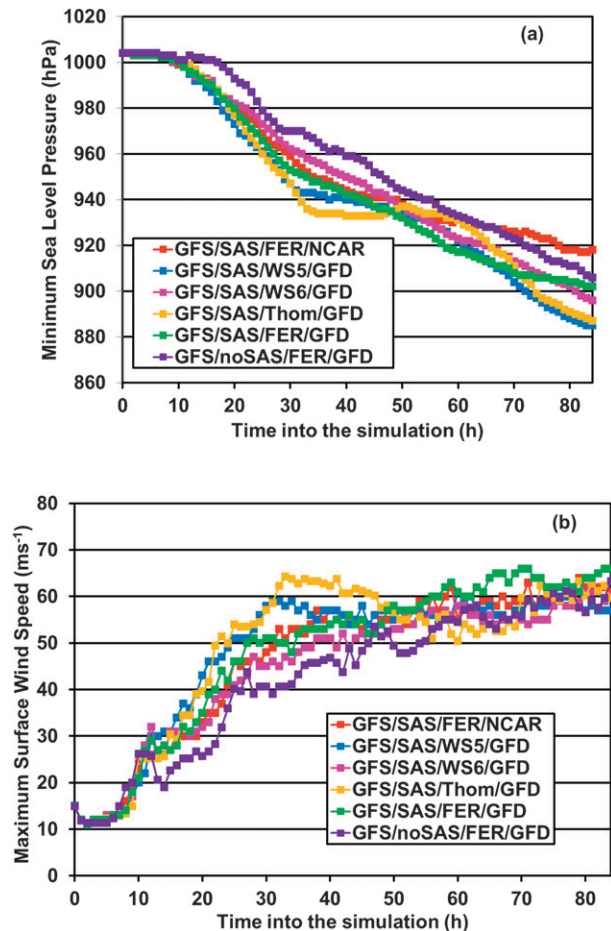

FIG. 9. (a) PMIN (hPa) and (b) VMAX (m s^{-1}). The red lines are expt 1, the blue lines are expt 7 (GFS/SAS/WSM5/GFDL schemes), the magenta lines are expt 8 (GFS/SAS/WSM6/GFDL schemes), the dark-yellow lines are expt 9 (GFS/SAS/Thom/GFDL schemes), the green lines are expt 10 (GFS/SAS/FER/GFDL schemes), and the purple lines are expt 11 (GFS/noSAS/FER/GFDL schemes).

intensity evolution of the simulated tropical cyclone is sensitive to the choice of microphysics scheme. In particular, the use of various microphysics schemes results in noticeable differences of both PMIN and VMAX, but smaller than those for BL or drag in the intensification rate of the simulated cyclone during the first 60 h of model integration. That is, the sensitivity shown in Fig. 9 is not as widespread as the other sensitivities shown previously. It is worth noting that exclusion of the subgrid convection scheme on the inner nest (experiment 11) reduces the intensification rate. This result is consistent with the finding reported by Zhu and Smith (2002) that a gestation period before the intensification is required to bring the boundary layer airflow near saturation, and the use of the parameterization scheme for subgrid convection helps shorten the
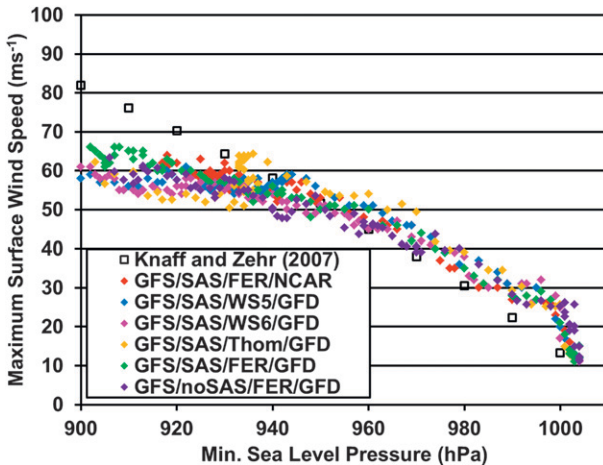
FIG. 10. Min sea level pressure vs max surface wind speed. The red filled diamonds are expt 1, the blue filled diamonds are expt 7, the magenta filled diamonds are expt 8, the dark-yellow filled diamonds are expt 9, the green filled diamonds are expt 10, the purple filled diamonds are expt 11, and the open squares are from Knaff and Zehr (2007).

gestation period before the intensification. As seen below, the exclusion of the SAS subgrid scheme on the inner nest also affects the structure of the simulated TC.

The PWR from experiments 7–10 appears (Fig. 10) to be more variable than that shown for the sensitivities to the BL mixing and the surface drag coefficient, particularly when the surface winds exceed 40 m s^{-1}. However, the scatter is comparable with the uncertainty in the mean PWR. These results indicate also that the variability of the simulated cyclone intensification with variations in the parameterized microphysics processes is comparable to the variability of the simulated intensification with variations in either the BL scheme or the surface drag coefficient. There are two quantitative aspects in the sensitivity results. First, different treatments of microphysical processes in the conversion of various hydrometeor species lead to different intensifications during the first 50 h of the model integration: the differences can be as big as, for example, 15 m s^{-1} between the WSM5 and WSM6 schemes at 30 h into the simulation. Second, the differences in the fluctuation of VMAX after the simulated vortex reaches the quasi-steady state (from 50 h on into the simulation) can be as big as 10 m s^{-1}. However, like the other experiments, VMAXs from these experiments are all smaller than that shown in - Knaff and Zehr (2007) for PMIN < 940 hPa, but greater for PMIN > 950 hPa. However, the scatter shown in the model-simulated PWRs has a similar magnitude to that of the uncertainty in the datasets used to obtain the Knaff and Zehr (2007) PWR (about

10 m s^{-1}). Therefore, there is again a need to use other metrics to more precisely discriminate the sensitivities.

Figure 11 shows the Hovmöller diagrams of the azimuthally averaged hourly tangential wind speed at 1 km above the surface from 0 to 84 h for the five experiments. It appears that in addition to the overall intensity, the variation in the microphysics scheme significantly affects the structural characteristics of the simulated cyclone. The differences in the characteristics of the azimuthally averaged tangential wind are noticeable and, particularly when comparing with Fig. 3a, the structural and intensity evolution of the tangential winds as characterized by the RMW and the 35 m s^{-1} contour show noticeable sensitivity to the choice of microphysics scheme used. Since the differences in the structural evolution shown among these experiments are comparable to those discussed in section 4a between experiments 4 and 5 (Fig. 3), one can conclude that the influence of the variation in the radiation scheme on the simulated cyclone development depends on the choice of microphysics scheme. This can be explained by the fact that different microphysics schemes produce different vertical distributions of hydrometeors in clouds, leading to variation in the simulated interaction of clouds and radiation, as elaborated on by Fovell et al. (2010).

Figure 12 shows the 60–72-h averaged radius–height cross sections of the tangential wind superimposed on the vectors of the secondary circulation, the radial wind speed, and the net forcing in the tangential direction. Overall, different microphysics schemes produce noticeable differences in the structures of tangential wind speed in terms of the shape of the area enclosed by the 30 m s^{-1} contour in spite of rather small differences in VMAX. Also, the use of different microphysics schemes appears to affect the radius of the maximum winds near the surface, possibly because of the cloud–radiation feedback effect on the vortex structure as revealed by Fovell et al. (2010). Comparing all five experiments, it is clearly seen that, relative to the Ferrier microphysics scheme, the other microphysics schemes produce smaller tangential acceleration in the low-level inflow and more deceleration above the inflow in the eyewall region, resulting in different characteristics of the low-level inflow and of the outflow in the eyewall region. It appears that variations in the microphysics scheme have a stronger impact on the secondary circulation than variations in either the BL scheme or the surface drag coefficient. The impact of the microphysics on VMAX appears to be less than that on the structure.

The sensitivity of the simulated tropical cyclone development to variation in the microphysics scheme can also be interpreted in terms of the role of diabatic heating in the development and maintenance of the secondary
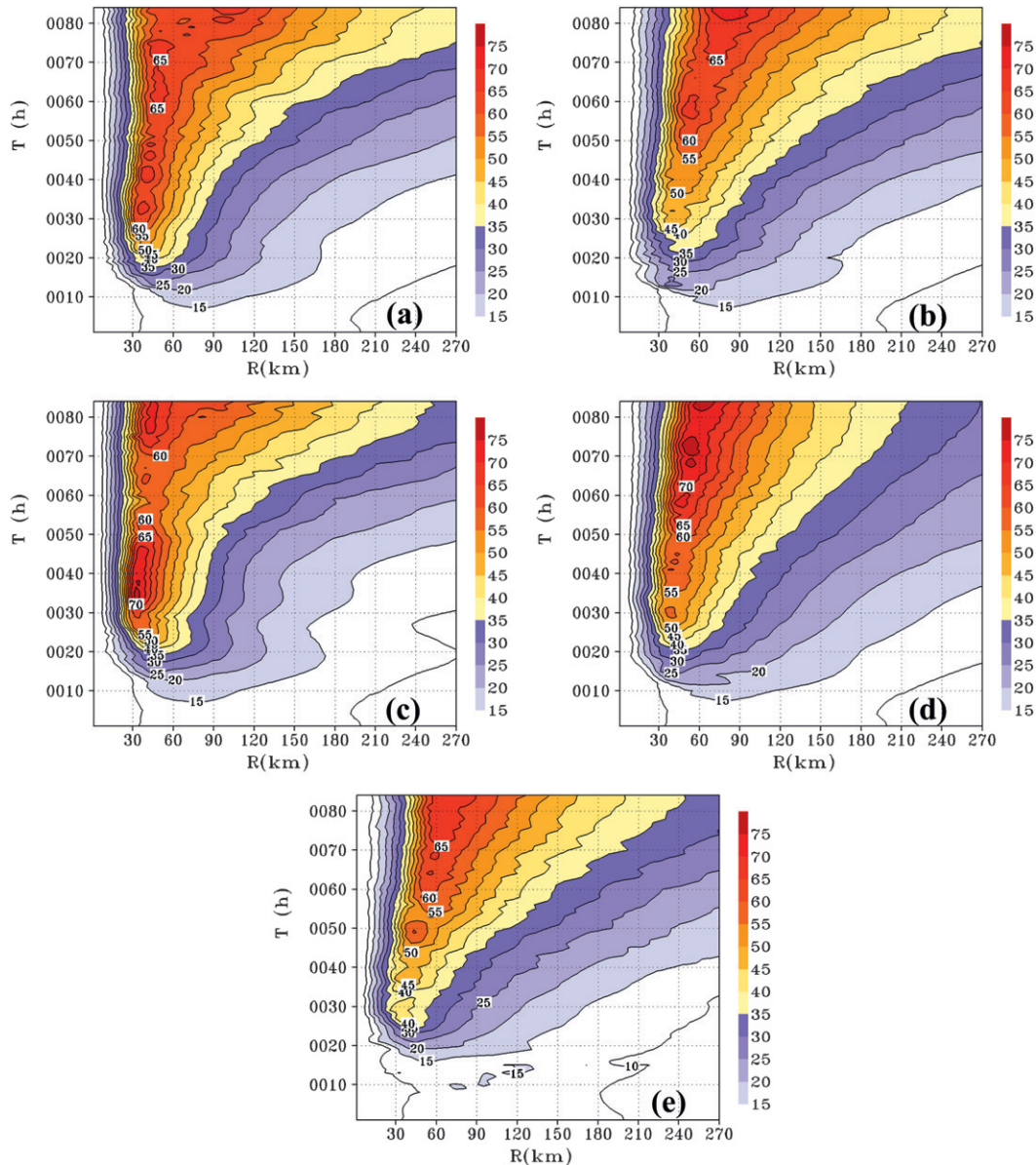
FIG. 11. As in Fig. 3, but for (a) expt 7, (b) expt 8, (c) expt 9, (d) expt 10, and (e) expt 11.

circulation according to the overview provided in section 3. It can be seen in Fig. 13 that even though all the experiments produce a thermal structure qualitatively similar to the well-recognized characteristics of a warm core vortex (see, e.g., Houze 2010), there are great differences in the details of the distribution of θ_e, relative humidity, and moisture flux when different microphysics schemes are used. Particularly, the distributions of latent heating, as indicated by the 98% relative humidity and 7 g m^{-2} s^{-1} contours of moisture fluxes that serve as the proxy for the maximum diabatic heating, are drastically different among the five experiments.

Careful examination of the spinup of the simulated vortex (not shown) indicates that the aforementioned differences in the diabatic heating distribution are due to the differences in the evolution of spiral rainbands outside the eyewall among the five experiments. Wang (2009) and Xu and Wang (2010a,b) revealed that the diabatic heating outside the eyewall strongly influences the overall intensity and structure of the simulated TC.

It is quite interesting to note that there are more differences in experiments 7–11 in terms of the structure than in terms of VMAX, PMIN, and PWR. This can possibly be interpreted by factors affecting the
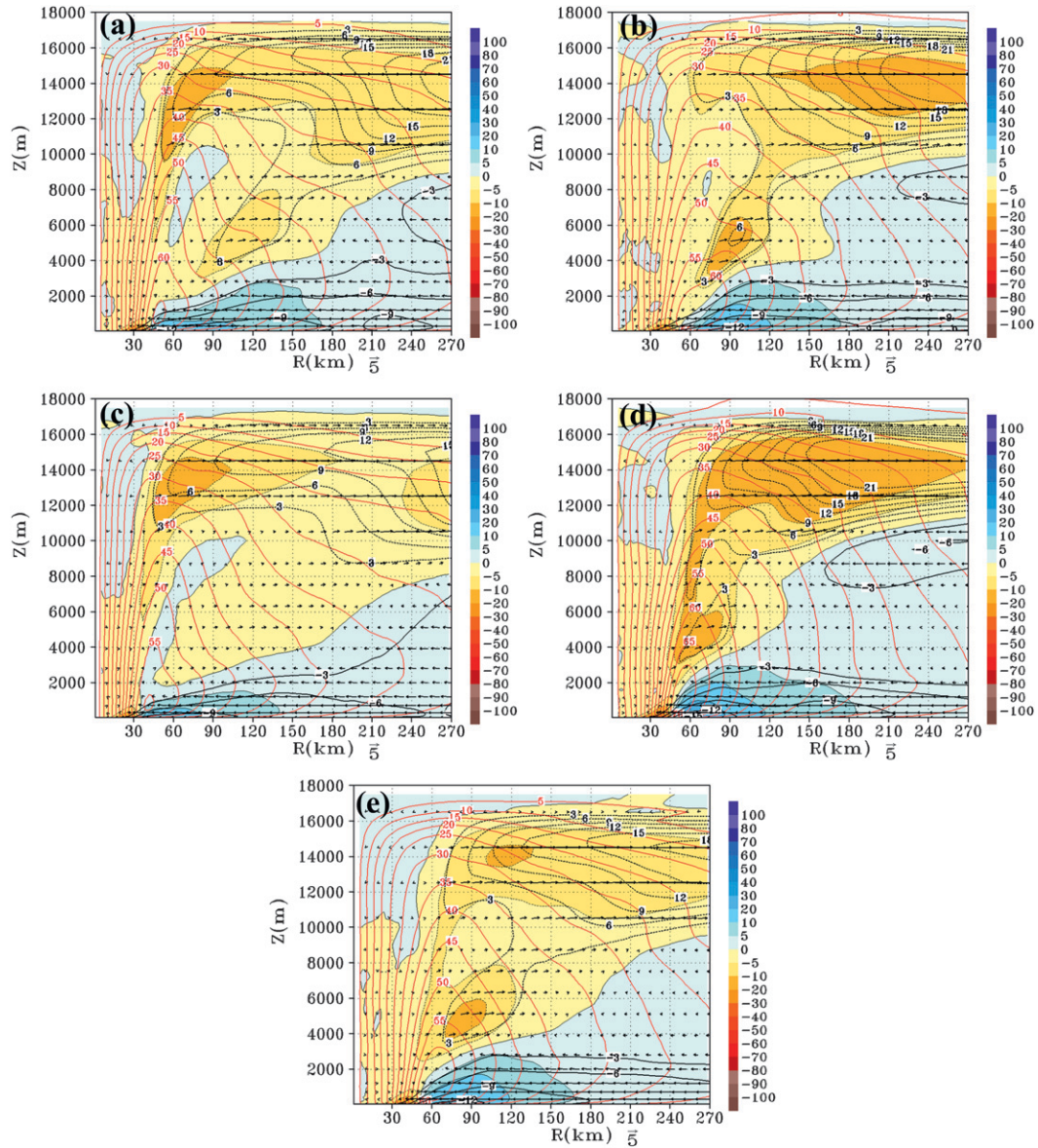
FIG. 12. As in Fig. 4, but for (a) expt 7, (b) expt 8, (c) expt 9, (d) expt 10, and (e) expt 11.

amplitudes of low-wavenumber eyewall asymmetries and the areal coverage of the surface sensible and latent heat fluxes. As shown by Fierro et al. (2009), for example, smaller amplitudes of low-wavenumber eyewall asymmetries and larger thermal radial gradients are favorable for tropical cyclone intensification in terms of VMAX and PMIN, while smaller surface fluxes limit the intensification. The smaller differences among experiments 7–11 in terms of VMAX, PMIN, and PWR strongly suggest that the differences in the microphysics schemes must have produced compensating differences in the structural properties and the surface fluxes, causing the changes in VMAX, PMIN, and PWR to be

relatively smaller for different microphysics schemes than the noticeable structural differences.

The drastic differences shown in Fig. 13 can also be understood dynamically as the differences in the response of a balanced axisymmetric vortex to different horizontal and vertical forcing distributions. Diabatic heating distribution is the result of the interaction between the cloud physics representation (including the subgrid component) and the dynamical model's response to diabatic heating realized by the cloud physics representation. Such a response can be described by diagnostic solutions of Eliassen's balanced vortex equations (see, e.g., Shapiro and Willoughby 1982; Bui
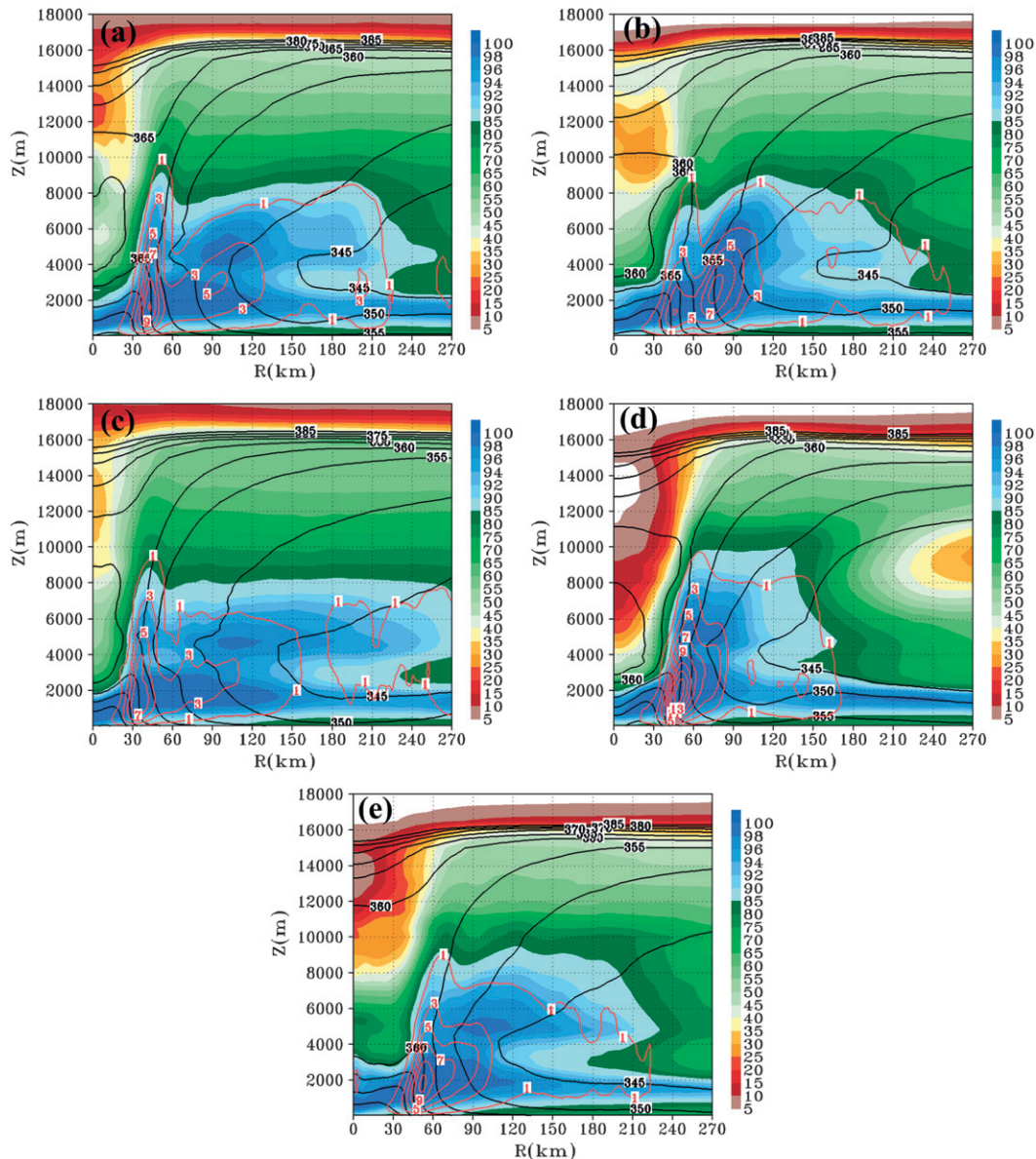
FIG. 13. The azimuthally and 60–72-h averaged radius–height cross section of RH (shaded colors), θ_e (black contours), and moisture fluxes (red contours) for (a) expt 7, (b) expt 8, (c) expt 9, (d) expt 10, and (e) expt 11.

et al. 2009; section 2 of MOSM). The dynamic nature of the response is summarized as the following: a forcing above the surface, such as diabatic heating and turbulent mixing of momentum, induces a transverse circulation around the source. Two circulations will form around the forcing in which ascent occurs in the center with return subsidence immediately outside; an inflow layer and an outflow layer will be established. Parcels leaving a forcing region are able to move horizontally or vertically depending on the inertial and static stabilities and baroclinicity. Strong inertial and static stabilities will constrain the circulation to near the vicinity of the

forcing. Baroclinicity will tilt the transverse circulation as parcels tend to follow the sloping isentropic surfaces (as a response to a momentum forcing) or the angular momentum surfaces (as a response to heating). The feedback of cloud–radiation interaction and the surface forcing associated with the surface drag and buoyancy flux can further distort the circulations (see, e.g., Fovell et al. 2010; Smith et al. 2011, manuscript submitted to *Quart. J. Roy. Meteor. Soc.*). Thus, the sensitivity of the HWRFX model–simulated tropical cyclone intensification simply reflects the dependence of the primary and secondary circulations on variations in the

diabatic heating and its feedback with vertical moisture flux associated with different microphysics schemes. Such dependence is dynamically intrinsic and has been revealed in TC simulations using models other than the HWRFX (see, e.g., Fovell and Su 2007; Fovell et al. 2009), particularly in a series of studies by Wang (2009), Hill and Lackmann (2009), Xu and Wang (2010a,b), and Fudeyasu and Wang (2011) on how the outer rainbands affect the simulated TC intensity and structure.

5. Summary and discussion

In this study, a series of idealized experiments with the HWRFX are performed with a horizontal grid spacing of 3 km (nested within a much larger 9-km parent domain). The purpose of the experiments is to reveal how sensitive the HWRFX is to commonly used microphysics, boundary layer, and radiation parameterization schemes. The sensitivity results are examined using various metrics in terms of VMAX and PMIN and the azimuthally averaged structural characteristics of the primary and secondary circulations.

Three major results are obtained from the comparisons of the sensitivity experiments. First, different boundary layer physics parameterization schemes for vertical subgrid turbulence mixing lead to differences not only in the intensity evolution in terms of VMAX and PMIN, but also in the structural characteristics of the simulated tropical cyclone. Second, the surface drag coefficient is a key parameter that controls the PWR and the agradient force near the surface. Third, different microphysics and subgrid convection parameterization schemes, because of different realizations of the diabatic heating distribution, lead to significant variations in the vortex structure. All of these results indicate that the current uncertainties in the BL mixing, surface drag, and microphysics parameterization schemes have comparable impacts on the intensity and structure of the HWRFX-simulated tropical cyclones.

These findings suggest that the differences of the sensitivity experiments measured in terms of VMAX and PMIN, along with the corresponding PWR, are not as revealing as the structural metrics in terms of azimuthally averaged tangential winds and the secondary circulation. The structural metric of the azimuthally averaged radii of maximum tangential winds appears to be much more effective in highlighting the sensitivity of the model-simulated tropical cyclone intensity to variations in physics parameterization schemes. In fact, structural metrics have long been used in the research community for research model verifications using reanalysis products along with measurements obtained from various observational instruments such as radars, satellites, and dropsondes, while operational models have long been evaluated only in terms of VMAX and PMIN. These findings illustrate the drawback of using the operational metrics of VMAX and PMIN to evaluate the performance of the HWRFX because they are not representative of the structure of the model-simulated cyclones. Practically speaking, the details of the model-simulated structure are important for forecasting coastal and inland flooding. While VMAX and PMIN are used widely as the essential parameters for verification of operational tropical cyclone forecasts, this study clearly demonstrates that other metrics are essential to evaluate dynamical impacts associated with the change in model physics. We therefore suggest that to effectively evaluate and provide useful recommendations for HWRF model improvement, structural metrics should be used in addition to operational metrics. These structural metrics should not be restricted to the ones in terms of azimuthal means that we have used in this study, and they should enable the use of all available observations of TC structure.

The sensitivity results reported herein can be understood largely from the axisymmetric perspective of the two coexisting and mutually dependent mechanisms of the idealized tropical cyclone spinup process: the radial convergence of absolute angular momentum above the BL driven by the convection in the eyewall region and the radial convergence of absolute angular momentum within the BL induced by the vortex intensification above the BL. That is, diabatic heating in the eyewall region induces convergence above the BL and intensifies the primary circulation because of the conservation of absolute angular momentum. As the axisymmetric vortex above the BL intensifies, the presence of surface friction induces radial inflow in the BL, which generally strengthens as parcels are accelerated down the radial pressure gradient toward the developing eyewall. Depending on the relative strength of the frictional torque and the generalized Coriolis force, the increasing radial inflow may generate a tangential wind that is stronger than that found above the boundary layer despite the loss of absolute angular momentum en route to the eyewall. The second spinup mechanism becomes progressively more important as the vortex develops and cannot be captured by axisymmetric balanced dynamics. From this perspective, the sensitivity of the HWRFX-simulated tropical cyclone intensification shown here simply reflects the dynamical dependence of the primary and secondary circulations on variations in the boundary layer and diabatic forcing associated with different physics parameterization schemes. Such a perspective points to the usefulness of using metrics beyond

VMAX and PMIN for the evaluation of this and other operational models.

The availability of high-performance computers at a relatively low cost now makes it possible to numerically forecast tropical cyclones in near–real time with complex physics parameterizations at a horizontal grid resolution on the order of 1 km. It is also tempting for models suitable for operational tropical cyclone prediction to be run at horizontal grid resolutions on the order of a few hundred meters for process studies. However, there remains a question as to how the quantitative aspects of the results from model sensitivity studies such as this one are affected as the model resolution increases. More importantly, whether or not the model solution with the current physics configuration will eventually converge as the model resolution continues increasing is still a subject of research. Nevertheless, the results from this study indicate that there is a need for developing a physically sound strategy to answer the following question: given the availability of various choices of physics parameterizations, what is the ''optimal combination'' of physics parameterizations in operational numerical models that should be used to forecast tropical cyclone intensity?

The current inability to evaluate the simulated structure of tropical cyclones using observations makes it difficult to determine the optimal choice of physics parameterizations. This difficulty has implications for the predictability of tropical cyclone intensification using current models. To tackle the difficulty, research and operational communities would be required to expand the current metrics of model evaluation to include structural parameters that can be reliably derived from observations. Some early efforts could be focused on using available observations from the past operational reconnaissance measurement and field programs such as the Coupled Boundary Layers Air–Sea Transfer (CBLAST) experiment. These observations might enable one to identify what is needed to modify the current operational HWRF model physics package to yield a physically sound structure as well as intensity without degrading the track prediction. When it is possible to tailor future observations to better meet specifics for operational model physics package improvement, more rigorous assessments would be required to identify and overcome fundamental shortcomings of the operational HWRF model physics through combined observational and modeling studies.

REFERENCES

Black, P. G., and Coauthors, 2007: Air–sea exchange in hurricanes: Synthesis of observations from the Coupled Boundary Layer Air–Sea Transfer experiment. *Bull. Amer. Meteor. Soc.,* **88,** 357–374.

Braun, S. A., and W.-K. Tao, 2000: Sensitivity of high-resolution simulations of Hurricane Bob (1991) to planetary boundary layer parameterizations. *Mon. Wea. Rev.,* **128,** 3941–3961.

Brown, D. P., J. L. Beven, J. L. Franklin, and E. S. Blake, 2010: Atlantic hurricane season of 2008. *Mon. Wea. Rev.,* **138,** 1975–2001.

Bryan, G. H., and R. Rotunno, 2009: The maximum intensity of tropical cyclones in axisymmetric numerical model simulations. *Mon. Wea. Rev.,* **137,** 1770–1789.

Bui, H. H., R. K. Smith, M. T. Montgomery, and J. Peng, 2009: Balanced and unbalanced aspects of tropical cyclone intensification. *Quart. J. Roy. Meteor. Soc.,* **135,** 1715–1731.

Craig, G. C., and S. L. Gray, 1996: CISK or WISHE as a mechanism for tropical cyclone intensification. *J. Atmos. Sci.,* **53,** 3528–3540.

Donelan, M. A., B. K. Haus, N. Reul, W. J. Plant, M. Stiassnie, H. C. Graber, O. B. Brown, and E. S. Saltzman, 2004: On the limiting aerodynamic roughness of the ocean in very strong winds. *Geophys. Res. Lett.,* **31,** L18306, doi:10.1029/2004GL019460.

Emanuel, K. A., 1995: Sensitivity of tropical cyclones to surface exchange coefficients and a revised steady-state model incorporating eye dynamics. *J. Atmos. Sci.,* **52,** 3969–3976.

Fierro, A. O., R. F. Rogers, F. D. Marks, and D. S. Nolan, 2009: The impact of horizontal grid spacing on the microphysical and kinematic structures of strong tropical cyclones simulated with the WRF-ARW model. *Mon. Wea. Rev.,* **137,** 3717–3743.

Fovell, R. G., and H. Su, 2007: Impact of cloud microphysics on hurricane track forecasts. *Geophys. Res. Lett.,* **34,** L24810, doi:10.1029/2007GL031723.

——, K. L. Corbosiero, and H.-C. Kuo, 2009: Cloud microphysics impact on hurricane track as revealed in idealized experiments. *J. Atmos. Sci.,* **66,** 1764–1778.

——, ——, A. Seifert, and K.-N. Liou, 2010: Impact of cloud-radiative processes on hurricane track. *Geophys. Res. Lett.,* **37,** L07808, doi:10.1029/2010GL042691.

French, J. R., W. M. Drennan, J. A. Zhang, and P. G. Black, 2007: Turbulent fluxes in the hurricane boundary layer. Part I: Momentum flux. *J. Atmos. Sci.,* **64,** 1089–1102.

Fudeyasu, H., and Y. Wang, 2011: Balanced contribution to the intensification of a tropical cyclone simulated in TCM4: Outer-core spinup process. *J. Atmos. Sci.,* **68,** 430–449.

Gopalakrishnan, S. G., F. Marks Jr., X. Zhang, J.-W. Bao, K.-S. Yeh, and R. Atlas, 2011a: The experimental HWRF system: A study on the influence of horizontal resolution on the structure and intensity changes in tropical cyclones using an idealized framework. *Mon. Wea. Rev.,* **139,** 1762–1784.

——, R. Rogers, X. Zhang, K. Yeh, T. Quirino, J.-W. Bao, and F. Marks, cited 2011b: TC structure and intensity research using HWRFx modeling system. [Available online at http://www.ofcm.gov/ihc10/Presentations/Session08/s08-03HWRFx_update_Marks_v3.ppt.]

Gray, W. M., E. Ruprecht, and R. Phelps, 1975: Relative humidity in tropical weather systems. *Mon. Wea. Rev.,* **103,** 685–690.

Harper, B. A., 2002: Tropical cyclone parameter estimation in the Australian region: Wind–pressure relationships and related issues for engineering planning and design—A discussion paper. Systems Engineering Australia Party Ltd. for Woodside Energy Ltd., SEA Rep. J0106-PR003E, 83 pp.

Hausman, S. A., 2001: Formulation and sensitivity analysis of a nonhydrostatic, axisymmetric tropical cyclone model.

Atmospheric Science Paper 701, Dept. of Atmospheric Science, Colorado State University, 210 pp.

Hill, K. A., and G. M. Lackmann, 2009: Influence of environmental humidity on tropical cyclone size. *Mon. Wea. Rev.,* **137,** 3294–3315.

Holland, G., 2008: A revised hurricane pressure–wind model. *Mon. Wea. Rev.,* **136,** 3432–3445.

Houze, R. A., Jr., 2010: Clouds in tropical cyclones. *Mon. Wea. Rev.,* **138,** 293–344.

Janjić, Z. I., 1994: The step-mountain Eta coordinate model: Further developments of the convection, viscous layer, and turbulence closure schemes. *Mon. Wea. Rev.,* **122,** 927–945.

——, 1996: The surface layer in the NCEP Eta Model. *Proc. 11th Conf. on Numerical Weather Prediction,* Norfolk, VA, Amer. Meteor. Soc., 354–355.

——, 2000: Comments on ''Development and evaluation of a convection scheme for use in climate models.'' *J. Atmos. Sci.,* **57,** 3686.

——, 2002: Nonsingular implementation of the Mellor–Yamada level 2.5 scheme in the NCEP Meso model. NCEP Office Note 437, 61 pp.

Jordan, C. L., 1958: Mean soundings for the West Indies area. *J. Meteor.,* **15,** 91–92.

Kepert, J. D., 2012: Choosing a boundary layer parameterization for tropical cyclone modeling. *Mon. Wea. Rev.,* **140,** 1427–1445.

Knaff, J. A., and R. M. Zehr, 2007: Reexamination of tropical cyclone wind–pressure relationships. *Wea. Forecasting,* **22,** 71–88.

Koba, H., T. Hagiwara, S. Asano, and S. Akashi, 1990: Relationships between CI number from Dvorak's technique and minimum sea level pressure or maximum wind speed of tropical cyclone. *J. Meteor. Res.,* **42,** 59–67.

Kossin, J. P., and C. S. Velden, 2004: A pronounced bias in tropical cyclone minimum sea level pressure estimation based on the Dvorak technique. *Mon. Wea. Rev.,* **132,** 165–173.

Liu, Y., D.-L. Zhang, and M. K. Yau, 1999: A multiscale numerical study of Hurricane Andrew (1992). Part II: Kinematics and inner-core structures. *Mon. Wea. Rev.,* **127,** 2597–2616.

Lord, S. J., H. E. Willoughby, and J. M. Piotrowicz, 1984: Role of a parameterized ice-phase microphysics in an axisymmetric, nonhydrostatic tropical cyclone model. *J. Atmos. Sci.,* **41,** 2836–2848.

Marks, F. D., Jr., R. A. Houze Jr., and J. F. Gamache, 1992: Dual-aircraft investigation of the inner core of Hurricane Norbert. Part I: Kinematic structure. *J. Atmos. Sci.,* **49,** 919–942.

Montgomery, M. T., M. E. Nicholls, T. A. Cram, and A. B. Saunders, 2006: A vortical hot tower route to tropical cyclogenesis. *J. Atmos. Sci.,* **63,** 355–386.

——, R. K. Smith, and S. V. Nguyen, 2010: Sensitivity of tropical cyclone models to the surface exchange coefficients. *Quart. J. Roy. Meteor. Soc.,* **136,** 1945–1953.

Nguyen, S. V., R. K. Smith, and M. T. Montgomery, 2008: Tropical cyclone intensification and predictability in three dimensions. *Quart. J. Roy. Meteor. Soc.,* **134,** 563–582.

Ooyama, K. V., 1982: Conceptual evolution of the theory and modeling of the tropical cyclone. *J. Meteor. Soc. Japan,* **60,** 369–380.

Pan, H.-L., and W.-S. Wu, 1995: Implementing a mass flux convective parameterization package for the NMC medium range forecast model. NMC Office Note 409, 40 pp. [Available

online at http://www.emc.ncep.noaa.gov/officenotes/FullTOC. html#1990.]

Powell, M. D., P. J. Vickery, and T. A. Reinhold, 2003: Reduced drag coefficient for high wind speeds in tropical cyclones. *Nature,* **422,** 279–283.

Schubert, H. V., and J. J. Hack, 1982: Inertial stability and tropical cyclone development. *J. Atmos. Sci.,* **39,** 1687–1697.

Shapiro, L. J., and H. E. Willoughby, 1982: The response of balanced hurricanes to local sources of heat and momentum. *J. Atmos. Sci.,* **39,** 378–394.

Skamarock, W. C., J. B. Klemp, J. Dudhia, D. O. Gill, D. M. Barker, W. Wang, and J. G. Powers, 2008: A description of the advanced research WRF version 3. NCAR Tech. Note NCAR/TN-475+STR, 113 pp.

Smith, R. K., and M. T. Montgomery, 2008: Balanced boundary layers in hurricane models. *Quart. J. Roy. Meteor. Soc.,* **134,** 1385–1395.

——, and S. Vogl, 2008: A simple model of the hurricane boundary layer revisited. *Quart. J. Roy. Meteor. Soc.,* **134,** 337–351.

——, and G. L. Thomsen, 2010: Dependence of tropical cyclone intensification on the boundary layer representation in a numerical model. *Quart. J. Roy. Meteor. Soc.,* **136,** 1671–1685.

——, M. T. Montgomery, and S. V. Nguyen, 2009: Tropical cyclone spin-up revisited. *Quart. J. Roy. Meteor. Soc.,* **135,** 1321–1335.

Wang, Y., 1995: An inverse balance equation in sigma coordinates for model initialization. *Mon. Wea. Rev.,* **123,** 482–488.

——, 2002: An explicit simulation of tropical cyclones with a triply nested movable mesh primitive equation model: TCM3. Part II: Model refinements and sensitivity to cloud microphysics parameterization. *Mon. Wea. Rev.,* **130,** 3022–3036.

——, 2009: How do outer spiral rainbands affect tropical cyclone structure and intensity? *J. Atmos. Sci.,* **66,** 1250–1273.

Weatherford, C. L., and W. M. Gray, 1988: Typhoon structure as revealed by aircraft reconnaissance. Part II: Structural variability. *Mon. Wea. Rev.,* **116,** 1044–1056.

Willoughby, H. E., 1979: Forced secondary circulations in hurricanes. *J. Geophys. Res.,* **84,** 3173–3183.

——, 1995: Mature structure and evolution. *Global Perspectives on Tropical Cyclones,* WMO/TD 693, R. L. Elsberry, Ed., World Meteorological Organization, 21–62.

Xu, J., and Y. Wang, 2010a: Sensitivity of tropical cyclone inner-core size and intensity to the radial distribution of surface entropy flux. *J. Atmos. Sci.,* **67,** 1831–1852.

——, and ——, 2010b: Sensitivity of the simulated tropical cyclone inner-core size to the initial vortex size. *Mon. Wea. Rev.,* **138,** 4135–4157.

Yamasaki, M., 1977: A preliminary experiment of the tropical cyclone without parameterizing the effects of cumulus convection. *J. Meteor. Soc. Japan,* **55,** 11–30.

Zhang, D.-L., Y. Liu, and M. K. Yau, 2001: A multiscale numerical study of Hurricane Andrew (1992). Part IV: Unbalanced flows. *Mon. Wea. Rev.,* **129,** 92–107.

Zhu, H., and R. K. Smith, 2002: The importance of three physical processes in a minimal three-dimensional tropical cyclone model. *J. Atmos. Sci.,* **59,** 1825–1840.